NONLINEAR WAVE TRANSFORMATION USING MODIFIED DISPERSIVE SHOALING MODELS

A Thesis

by

MOURYA PENUGONDA

Submitted to the Office of Graduate and Professional Studies of
Texas A&M University
in partial fulfillment of the requirements for the degree of

MASTER OF SCIENCE

Chair of Committee,	James M. Kaihatu
Committee Members,	Moo-Hyun Kim
	Jun Kameoka
Head of Department,	Robin L. Autenrieth

August 2018

Major Subject: Civil Engineering

ABSTRACT

This study is to compare and validate two models for random wave transformation with experimental data. Both models are based on frequency domain KdV equation. First model is a modified version of KdV equation which was derived to provide shoaling and dispersion relation of each frequency mode. Second model is a dispersive nonlinear shoaling model including shallow water limits and dissipation terms. Results expected are as follows 1) Second model is expected to overestimate the results in higher frequencies but can predict satisfactorily close in the lower and intermediate frequency zones of the energy spectrums. 2) First model is expected to predict the transformation better than that of the second because of the fully dispersive nature.

Energy spectrum plots from models are expected to match close to the experimental plots in the lower frequencies and the first model is expected to be much closer to the experimental data than that of the second model. The validation plots of both the models are expected to be as close as they can be in the Infra gravity and Swell regions of the spectrum; the second model is expected to do better in the Sea wave region of the spectrum.

DEDICATION

There is one person in my life to whom I can dedicate anything of mine without any doubt. I am planning to go for doctorate studies. But, if there is an opportunity to dedicate I am not going to let it go. So, I would like to dedicate this important part of my life to my mom. Even she doesn't know how much she deserves this. But when I say that I included her in thesis she will be happy and that's enough for me.

ACKNOWLEDGEMENTS

When I was looking for the placement of the Acknowledgements many sources mentioned that it is optional, but it is not at all an optional thing for me. I would like to thank for the opportunity and guidance Dr. Kaihatu my committee chair has provided. And I would also like to thank him for the summer 2017 student assistant opportunity which lead to this study.

I would like to thank my committee members who were guiding me and cooperating with the schedule as much as possible. I would like to acknowledge my gaming buddy Praneeth for distracting me and giving me a break from the research work. I would also like to thank my roommate and a very dear friend Bala for all the time he helped me have fun away from the studies which made my work look easy. Finally I would like to thank Civil and Ocean Engineering departments of Texas A&M university faculty and staff for maintaining a great learning and peaceful environment.

CONTRIBUTORS AND FUNDING SOURCES

All the work and research for the study is supervised by the chair of the committee Dr. James M. Kaihatu of Civil Engineering department. The data required, and previous versions of the models are also provided by Dr. Kaihatu. All work for the thesis was completed independently by the student.

This work was made possible in part by National Science Foundation under Grant Number 1538190. The grant was a collaborative research sponsored by Texas A&M Engineering Experimentation Station and CMMI a division of Civil, Mechanical, & Manufacturing Innovation. The main idea of the research was to study the Nonlinear long wave amplification in the shadow zone of offshore islands. Research contents are solely the responsibility of the authors and do not necessarily represent the official views of the National Science Foundation.

NOMENCLATURE

B/CS	Bryan/College Station
C.C.	Complex Counterpart
TAMU	Texas A&M University
OSU	Oregon State University
TWL	Tsunami Wave Lab
M1	Model one
M2	Model two
Expt.	Experiment or Experimental

TABLE OF CONTENTS

Page

LIST OF FIGURES

Page

LIST OF TABLES

1. INTRODUCTION

Waves approach a beach or a cliff while constantly changing their shapes and, in most cases, they break. The aim of the study is to establish a better model to best predict the wave transformation. The characteristics of wave transformation depend on the local bathymetry and on its variations, as water depth, affects the shoaling and refraction characteristics, frequency dispersion, and energy dissipation. Most commonly used shoaling wave theories and models are mainly based on linear wave theory.

While models based on linear theory are computationally fast, they do have drawbacks. Many of these models are based on the so-called WKB assumption, which impose that the change in water depth is small over a wavelength. These models predict surface elevation changes by conserving energy flux and calculating the changes in the parameters required for this to be maintained.

Linear wave models are sufficient if the goal is to predict lumped parameters such as significant wave height. However, for many processes this is insufficient. For example. the nonlinear aspects of the wave transformation are necessary to estimate the properties of sediment transport. Sediment transport mainly depends on the velocity of the particles, and skewness and asymmetry of the waves which are necessary for the pickup and transport of the particles. Nonlinear wave behavior is thus necessary to capture this effect.

Modern shallow water wave theory started with Peregrine (1967), who used the Boussinesq theory to model long waves with small amplitudes propogating in varying water depth. These equations are considered as an advancement to the linear wave theory.

Boussinesq equations can predict the transformation of monochromatic waves.. Boussinesq equations have only lowest order of nonlinearity and dispersion, and are thus considered weakly nonlinear and weakly dispersive. The treatment of nonlinearity, however, is quite different than classic Stokes waves.

Ursell (1953) had demonstrated that Stokes perturbation solutions to address nonlinearity were valid only for Ursell number $\frac{a\lambda^2}{h^3} \ll 1$ and that the shallow water approximated equations are valid for $\frac{a\lambda^2}{h^3} \gg 1$, where λ is length scale or wave length, h is the water depth and a is the water surface elevation.

Scholars came up with better approach to address these problem with the help of frequency domain analysis. Slowly varying, linear, finite-depth theory is roughly consistent with observations of root mean square shoaling wave heights, but some spectral features are apparently due to nonlinear effects (Guza & Thronton 1980). The Korteweg de Veris and Boussinesq equations are extended to improve damping and dispersion characteristics. It was always obviously clear that the wave braking process is nonlinear by nature.

Freilich and Guza (1984) came up with the “consistent shoaling model” from the one dimensional Boussinesq euation. Mase and Kirby (1992) developed a hybrid model to predict the transformation by modifying the KdV equation and including both fully dispersive linear shoaling, shallow water nonlinearity and a damping coefficient in the equation to represent breaking.

The initial models did not predict the energy content in the high frequency region of the spectrum because of the degree of nonlinearity is low and the shoaling properties

are neglected an extent. So, these models are expected to show how adding the shoaling and dissipation to the equation gives a better prediction of the transformation. In this study two nonlinear models for the transformation of waves in special regions are focused on. The models predict both cross spectral energy and nonlinear modal phase changes. In the experimental section details of wave parameters collected and data processing along with the conditions under which they ae collected is explained. Measurements are compared with the two models for all the wave conditions in experimental section and conclusions are drawn.

2. PROBLEM AND BACKGROUND

In this section of the thesis the advancements over linear wave theory and the reasons for the advancement that resulted in this study will be discussed.

Starting with the boundary value problem to solve for the potential $\phi\ in\ (x, y, z)$coordinate system. We consider water depth h that is slowly varying and relatively small amplitude η waves.

$$\nabla^2\phi = \nabla^2{}_h\phi + \phi_{zz} = 0 \qquad \text{for} \qquad -h \le z \le \eta \tag{2.1.a}$$

$$\phi_z = -\nabla_h h.\nabla_h\phi \qquad \text{for} \qquad z = -h \tag{2.2.a}$$

$$g\eta + \phi_t + \tfrac{1}{2}(\nabla_h\phi)^2 + \tfrac{1}{2}(\phi_z)^2 = 0 \qquad \text{for} \qquad z = \eta \tag{2.3.a}$$

$$\eta_t - \phi_z + \nabla_h\eta.\nabla_h\phi = 0 \qquad \text{for} \qquad z = \eta \tag{2.4.a}$$

where subscripts denote differentiation with respect to that parameter. These equations are approximated using Taylor series expansion from z = 0 as starting point and retaining the terms to the second order nonlinearity (O (ε^2)) where $\varepsilon = ka$ is the nonlinearity parameter, *k* is the wave number and *a* is amplitude of wave. The truncated version is as following

$$\nabla^2{}_h\phi + \phi_{zz} = 0 \qquad \text{for} \quad -h \le z \le 0 \tag{2.1.b}$$

$$\phi_z = -\nabla_h h.\nabla_h\phi \qquad \text{for} \qquad z = -h \tag{2.2.b}$$

$$g\eta + \phi_t + \tfrac{1}{2}(\nabla_h\phi)^2 + \tfrac{1}{2}(\phi_z)^2 + \eta\phi_{zt} = O(\varepsilon^2) \quad \text{for} \qquad z = 0 \tag{2.3.b}$$

$$\eta_t - \phi_z + \nabla_h\eta.\nabla_h\phi - \eta\phi_{zz} = O(\varepsilon^2) \qquad \text{for} \qquad z = 0 \tag{2.4.b}$$

A superpositioned solution is assumed for the potential

$$\phi(x,y,z,t) = \sum_{n=1}^{N} f_n(k_n,h,z)\hat{\phi}_n(k_n,\omega_n,x,y,t) \tag{2.5}$$

where k_n is the wave number and ω_n is radian frequency of the n^{th} frequency component. Here $f_n = \frac{\cosh k_n(h+z)}{\cosh k_n h}$ and $k_n \; and \; \omega_n$ follow the linear dispersion relation

$$(n\omega)^2 = gk_n tanh(k_n h) \tag{2.6}$$

Combining the boundary conditions 2.3.b and 2.4.b and eliminating η from the equation, assuming slowly varying bottom slope and using the Green's second identity on the variables f_n and $\hat{\phi}_n$ Kaihatu and Kirby(1995) came up with the equation with nonlinear terms that oscillate near the frequency ω_n explained in Section 2.2.

$$\hat{\phi}_{tt} - \nabla_h.\left[\left(CC_g\right)_n \nabla_h\hat{\phi}_n\right] + \omega_n^2\left(1 - \frac{C_{gn}}{C_n}\right) = \frac{1}{2}\left\{\sum_l\sum_m\left[\frac{\omega_l^2+\omega_m^2}{g^2}\left(\hat{\phi}_{l_t}\hat{\phi}_{m_t}\right)_t - \right.\right.$$

$$\left.\left.\frac{\omega_l^2\omega_m^2}{g^2}\left(\hat{\phi}_l\hat{\phi}_m\right)_t\right] - \sum_l\sum_m\left[\left(\nabla_h\hat{\phi}_l.\nabla_h\hat{\phi}_m\right)_t + \nabla_h.\left(\hat{\phi}_{l_t}\nabla_h\hat{\phi}_m\right) + \nabla_h.\left(\hat{\phi}_{m_t}\nabla_h\hat{\phi}_l\right)\right]\right\}_n \tag{2.7}$$

Now by specifying the time dependence by assuming the following relation and parabolic approximation we derive the equation in Section 2.2.

$$\hat{\phi}_n(x,y,t) = \frac{\breve{\phi}_n}{2}e^{-i\omega_n t} + \frac{\breve{\phi}_n^*}{2}e^{i\omega_n t} \tag{2.8}$$

2.1 Peregrine (1967) Boussinesq Equations

Peregrine started with Euler equations along with asymptotic expansion of depending variables derived the surface elevation equation so that the second order variables are included. Using the Euler equations, vertical momentum equations with substitution of second order variable and averaging horizontal velocity over depth

conservation of mass equation (2.9) and an equation (2.10) for conservation of momentum are derived.

$$\eta_t + \nabla.(h+\eta)\bar{u} = 0 \tag{2.9}$$

$$\overline{u_t} + \bar{u}.\nabla_h\bar{u} + g\nabla_h\eta = \frac{h}{2}\nabla_h[\nabla_h.(h\overline{u_t})] - \frac{h^2}{6}\nabla_h[\nabla_h.\bar{u}] \tag{2.10}$$

where h is the water depth, η is the free surface elevation, $\bar{u}$ is the depth averaged horizontal velocity, ∇_hrepresents horizontal gradient operator in (x,y), and the subscript t denotes differentiation w,r,t time. Assuming plane one direction wave with η and $\bar{u}$ as

$$\eta = ae^{i(kx-\omega t)} \text{ and } \bar{u} = u_0 e^{i(kx-\omega t)} \tag{2.11}$$

Solving these "standard" Boussinesq equations (2.11) result in the dispersion relation (2.12)

$$\omega^2 = \frac{gk^2h}{\left[1+\frac{1}{3}(kh)^2\right]} \approx gk^2h\left[1-\frac{(kh)^2}{3}\right] \tag{2.12}$$

where k is the wave number. This dispersion relation is basically the linear dispersion relation. These equations are useful and effective in predicting shallow water wave transformation. Adding damping and dissipation can better the prediction in the shoaling and the breaking regions. These equations fundamentally lack the frequency dependent dispersion nature which is a major characteristic in two-dimensional topography wave propagation and deep-water application. It has been studied that the Boussinesq equations based nonlinear wave shallow water models can be solved using time domain and frequency domain models. Korteweg-deVries (KdV) equations were used by Svendsen (1976) Liu et al. (1985) to give water surface elevation with flat bottom (2.13) and variable depth (2.14) were formulated respectively.

The KdV equations and Kadomtsev-Petviashvili (KP) equations have water surface elevation as their only dependent variable. For deriving these equations potential is used, and the coordinate system is moving with the speed of $\sqrt{gh}$. But the wave is not assumed to be study and the wave have some shift in time.

$$\frac{1}{C}\eta_t + \eta_x + \frac{h_x}{4h}\eta + \frac{3}{2h}\eta\eta_x + \frac{h^2}{6}\eta_{xxx} = 0 \tag{2.13}$$

$$\left(\frac{1}{C}\eta_t + \eta_x + \frac{h_x}{4h}\eta + \frac{3}{2h}\eta\eta_x + \frac{h^2}{6}\eta_{xxx}\right)_x + \frac{1}{2h}\left(h\eta_y\right)_y = 0 \tag{2.14}$$

where the subscripts x and y refer to differentiation w.r.t. x and y respectively. A second-degree nonlinearity is assumed and accounted for in these equations. Permanent form solutions for solitary and cnoidal waves were derived from these equations. The dispersion relation used in formulating these equations was

$$\omega = \sqrt{gh}k\left[1 - \frac{1}{6}(kh)^2\right] \tag{2.15}$$

where ω is frequency of the wave. This relation (2.7) is basically an approximated form of dispersion relation (2.16) from linear wave theory.

$$\omega^2 = gk\tanh kh \tag{2.16}$$

Boussinesq (1871) derived the set of evolution equations that contained weak dispersion terms due to finite depth, and weak nonlinearity due to finite amplitude. Korteweg-deVries (1895) followed with a single equation (KdV) describing a similar system supporting unidirectional wave motion only. These two equation are valid in the regime where the Ursell number is of order one (O(1)). Problem with all these models and these dispersions relations is that they converge in shallow water region and diverge at high *kh* values. All the models assumed close to linear conditions which are far from the

actual cases. So, these models are expected to work better in the regions where $kh<<1$. So, for the other regions better model was required. And frequency domain based nonlinear models provided the solution.

2.2 Fully Non-Linear Frequency domain models

Both KdV and Boussinesq equations were extended to improve damping and dispersion characteristics by Madsen, Murray, Sorensen and also Kangaonkar and LeMehaute (1991) in separate studies. Before that Freilich and Guza (1984) came up with the "consistent shoaling model" from fully dispersive nonlinear shoaling model which was the result of modified spectral KdV equation.

We should start with resonant triad interaction concept to move further in Freilich and Guza derivation. For going to derivation completely with frequency domain, periodicity in time was to be assumed and time dependency was removed. The basic assumption of Fourier transform says we assume that the random wave will repeat itself after we stop the time period or as long as we take the reading. This will allow us to formulate spatially varying amplitudes of wave components. Phillips (1977) discussed implications of triad resonance interaction which is basically shallow water resonance. Here waves are treated as periodic with some phase difference, varying amplitudes, and nonlinear effects come from resonance affects. Here complete resonance is assumed.

Armstrong et al. (I962) and Bretherton (1964) introduced the concept of 'near resonance' in weakly nonlinear systems with discrete spectra. They showed that, on moderate length or time scales, significant cross-spectral energy transfers and modal phase

modifications could take place if the resonance conditions were only approximately satisfied.

Using the following Fourier series representation of the surface elevation and resonance conditions, complex amplitudes are introduced into the equations (2.13 and 2.14).

$$\eta = \sum_{n=1}^{\infty} \frac{1}{2} A_n e^{in(\int k_1 dx - w_1 t)} + c.c. \quad (2.17.1)$$

Some of the product terms oscillate at n and they may follow the following combinations from the normal and conjugate terms.

$$n = l+m$$

$$n = l-m$$

$$n = m-l$$

$$n = -l-m$$

where *l, m* are any numbers from 1 to ∞. Taking above combinations that only oscillate in nth frequency and dividing the exponential parts the resulting equation is limited to *N* number of combinations.

Because of the shallow water assumption which gives the "consistent shoaling model".

$$\frac{dA_n}{dx} + \frac{h_x}{4h} A_n - \frac{in^3 {k_1}^3 h^2}{6} A_n + \frac{3ink_1}{8h} \left[\sum_{l=1}^{n-1} A_l A_{n-l} + 2\sum_{l=1}^{N-n} A_l{}^* A_{n+l}\right] = 0 \quad (2.17)$$

n = 1,2,3……..N

Liu et al, gave a 2D version of equation 2.17

$$2ink_0A_{nx} + \frac{k_0}{kG_n}\left(hA_{ny}\right)_y + \frac{A_n}{G_n}\left[\frac{ink_0}{2}G_{nx} - 2n^2k_0(k_0-k)G_n + \frac{n^2k_0\omega^4h}{3g^2k}\right] =$$

$$\frac{3n^2kk_0}{4G_n}\left(\sum_{l=1}^{n-1}A_lA_{n-l} + 2\sum_{l=1}^{N-n}A_l^*A_{n+l}\right) \qquad (2.18.1)$$

n = 1,2,3……..N

where k_0 is the constant reference wavenumber and G_n is a function defined as

$$G_n = h\left(1 - \frac{n^2\omega^2h}{3g}\right) \qquad (2.18.2)$$

where k_1 represents primary wave-number and w_1 represents primary frequency. N represents the number of equations that we wish to solve. Higher the N better the accuracy similarly, the complexity and the time to solve increases with increase in N. The equation is named consistent because of the nonlinearity in all the variable being at same order.

2.3 Mase and Kirby Hybrid Equation – Model one

Green's Law which defines the evolution of non-breaking surface waves propogating in shallow water of varying depth and width is used to modify the equation (2.18) also involving the fully dispersive shoaling linear theory.

$$\frac{dA_n}{dx} = -\frac{h_x}{4h}A_n \qquad (2.19)$$

Equation (2.19) is compared to the component of fully dispersive linear theory to give

$$\frac{dA_n}{dx} = -\frac{(C_{g_n})_x}{2C_{g_n}}A_n \qquad (2.20)$$

Which can be substituted back in the equation (2.18) to give

$$\frac{dA_n}{dx} + \frac{(C_{g_n})_x}{4C_{g_n}} A_n - ink_1 \left(\sqrt{\frac{k_n h}{\tanh k_n h}} - 1 \right) A_n \quad + \frac{3ink_1}{8h} [\sum_{l=1}^{n-1} A_l A_{n-l} +$$

$$2 \sum_{l=1}^{N-n} A_l{}^* A_{n+l}] = 0 \qquad (2.21)$$

n = 1,2,3,…….N

where C_g is the group-velocity. And for the calculation of group velocity by formula $C_{g_n} = \frac{n\omega}{2k_n} \left(1 + \frac{2k_n h}{\sinh(2k_n h)}\right)$ where $k_n$is calculated by the linear dispersion relation $(n\omega)^2 = gk_n tanh(k_n h)$. Here $n\omega = \omega_n$ and ω_n, k_n pair satisfy the lowest order dispersion relation. Some featured of this interaction show slow energy transfer between interacting modes, slow phase shifts among interacting modes though they are small in scale.

This resulted modified version of KdV equation with changed shoaling and dispersion terms give exact relation of each frequency mode. To the equation (2.21) energy dissipation and damping terms are added to get the first model in our study. The equation that our first model is based on is

$$\frac{dA_n}{dx} + \frac{(C_{g_n})_x}{4C_{g_n}} A_n - ink_1 \left(\sqrt{\frac{k_n h}{\tanh k_n h}} - 1 \right) A_n + \frac{3ink_1}{8h} [\sum_{l=1}^{n-1} A_l A_{n-l} + 2 \sum_{l=1}^{N-n} A_l{}^* A_{n+l}] +$$

$$\alpha_n A_n = 0 \qquad (2.22)$$

n = 1,2,3,……N

where α_n mostly is nearly constant for short distance and estimated using the spectral energy densities. It contains effects of shoaling and nonlinear wave interaction effects.

$$\sum_{n=1}^{N} [(S_n)_x + 2\alpha_n S_n] = 0 \qquad (2.23.1)$$

where Sn is the spectral density. Thornton and Guza (1983) formulated an expected value of energy dissipation rate based on the probabilistic method of Rayleigh distribution of waves height. This study gave an easy way to calculate α_n.

$$\alpha_n = \alpha_0 + \left(\frac{f_n}{\bar{f}}\right)^2 \alpha_1 \tag{2.23.2}$$

where $\alpha_0 \; and \; \alpha_1$ formulation is explained in the section 2.4.

2.4 Modified Fully Dispersive Shoaling model – Model two

Starting with Freilich and Guza's "consistent shoaling model" (2.18) the further modifications are done by adding a term that is equivalent to the undifferentiated dissipation term in the KdV equation (2.14). $\alpha_0 \; and \; \alpha_1$ are introduced to purpose of division of dissipation to frequency and frequency squared terms. Adding the dissipation term results in

$$\frac{dA_n}{dx} + \frac{h_x}{4h} A_n - \frac{in^3 {k_1}^3 h^2}{6} A_n + \frac{3ink_1}{8h} \left[\sum_{l=1}^{n-1} A_l A_{n-l} + 2\sum_{l=1}^{N-n} A_l{}^* A_{n+l}\right] + \left(\alpha_0 + \alpha_1 \left(\frac{n*df}{f_p}\right)^2\right) A_n = 0 \tag{2.24}$$

n = 1,2,3…..N

where $$\alpha_0 = e_p * \beta \tag{2.25}$$

$$\alpha_1 = (\beta - \alpha_0) * \left({f_p}^2\right) * \left(\frac{\sum_{n=1}^{N} abs(A_n)}{\sum_{n=1}^{N} df n^2 (abs(A_n))^2}\right) \tag{2.26}$$

$$\beta = \left[\left(\frac{3b^3 f_p \sqrt{\pi}}{4\gamma^4 \sqrt{g}}\right) / h^{5.5}\right] \sqrt[4]{4 \sum_{n=1}^{N} (A_n)^2} \tag{2.27}$$

where e_p is the parameter that specifies the dependence of dissipation on frequency. β is a function of "b" and "γ" parameter in the Thornton and Guza dissipation, peak frequency

f_p and depth h. The second model is designed based on the equation (2.24). α_0 represents uniform energy decay in all frequency components and α_1 denoted the f^2 dependence.

3. EXPERIMENTS AND SETUP

3.1 Experiments and Reason

The main reason that resulted in these experiments is a photograph of leading edge fission waves at Koh Pu island prior to the arrival of the 2004 tsunami. The image shows a leading edge marked by short waves and these short waves appeared to be cnoidal in shape. These waves also had temporal and spatial scale in line with the longest sea present in the region. So obviously the concern was the cause for this special case and its interaction with the random waves in the background of that picture.

Figure 1: 2004 Indian ocean tsunami near Koh Pu Island P.C. Anders Garwin.

For many years solitary waves were considered to be the proxy for tsunami waves. Because of these images and their contrary observations further study was needed to determine the characteristics of tsunami. So different combinations of cnoidal waves with random waves were used in the experiments.

3.2 Experimental Facility and Setup

The experiments were conducted at the Large Wave Flume in the O.H. Hinsdale Laboratory at Oregon State University during 2013-2014. The wavemaker is with a programmable hydraulic actuator capable of generating repeatable regular, irregular, tsunami, and user-defined waves. Main goal of the experiments was to determine the tsunami interaction with the oceanographic surroundings and the nearshore wave mechanics.

Figure 2: Large wave flume (LWF) bathymetry. P.C. OSU website.

Figure 3: Large wave flume (LWF) with waves at OSU. P.C. OSU website.

The bathymetry used in the models and in the experiment is explained and shown below. The profile has change in slope twice along the length. Minimum depth in profile is set to be one centimeter. Total length of the basin is set to be 58 meters in the model. Millimeter resolution is used in the simulation. A total of 18 wave gauges are used in the experiments. In which gauge 9 from the wave maker side was faulty.

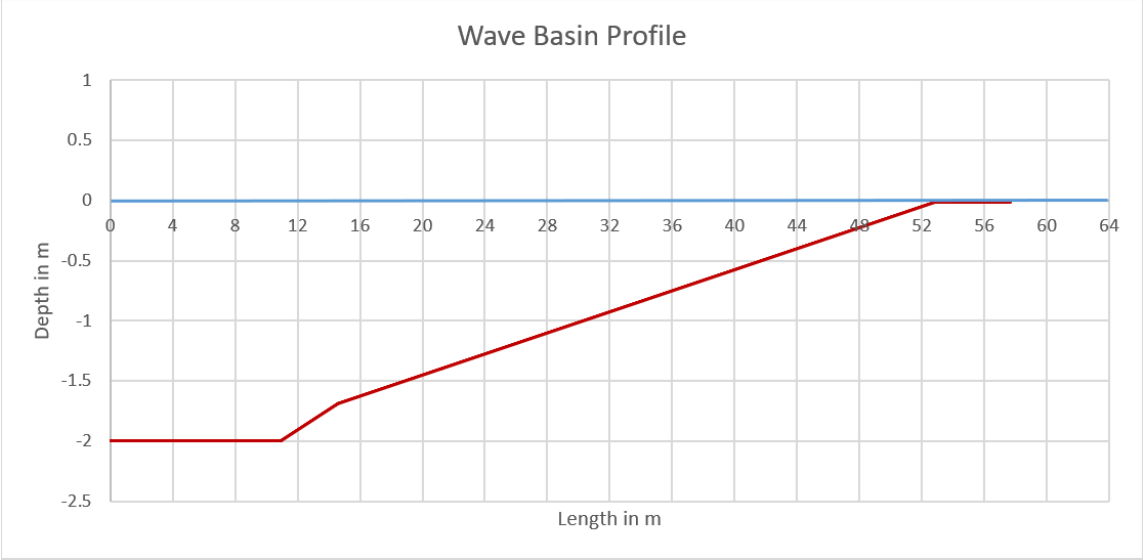

Figure 4: Wave basin profile with changing slope.

Depth profile		
X distance	Depth (from-to)	Slope
0.00 to 10.97 m	2.00 m	0
10.97 to 14.62 m	2.00 - 1.69 m	1:12
14.62 to 52.84 m	1.69 - 0.01 m	1:24
52.84 to 58 m	0.01 m	0

Table 1: Depth profile.

Gauge Location			
Gauge 0 (models only)	10 cm		
Gauge 1	3.65 m	Gauge 10	31.08 m
Gauge 2	7.32 m	Gauge 11	33.00 m
Gauge 3	10.96 m	Gauge 12	34.76 m
Gauge 4	14.62 m	Gauge 13	36.57 m
Gauge 5	18.28 m	Gauge 14	38.40 m
Gauge 6	21.94 m	Gauge 15	40.35 m
Gauge 7	25.70 m	Gauge 16	41.98 m
Gauge 8	27.41 m	Gauge 17	43.99 m
Gauge 9	29.34 m	Gauge 18	46.00 m

Table 2: Gauge locations from the self-calibrating wave gauge.

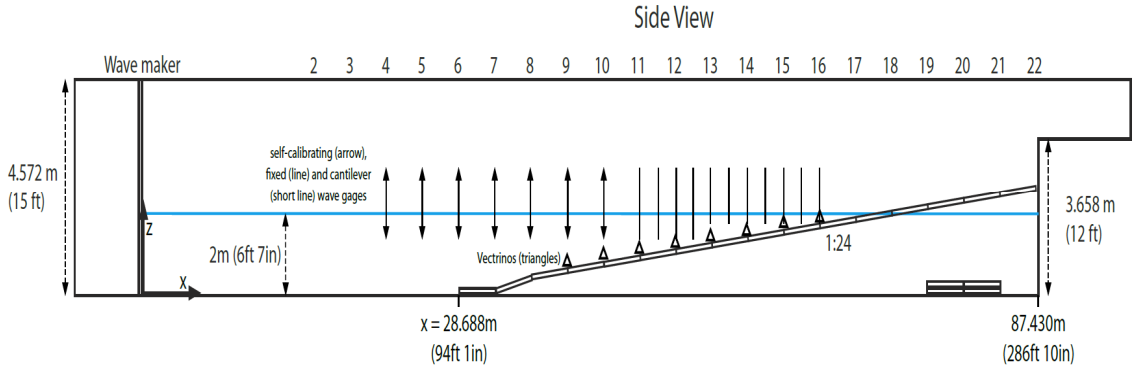

Figure 5: Gauge (1-18) locations with basin profile in experiments.

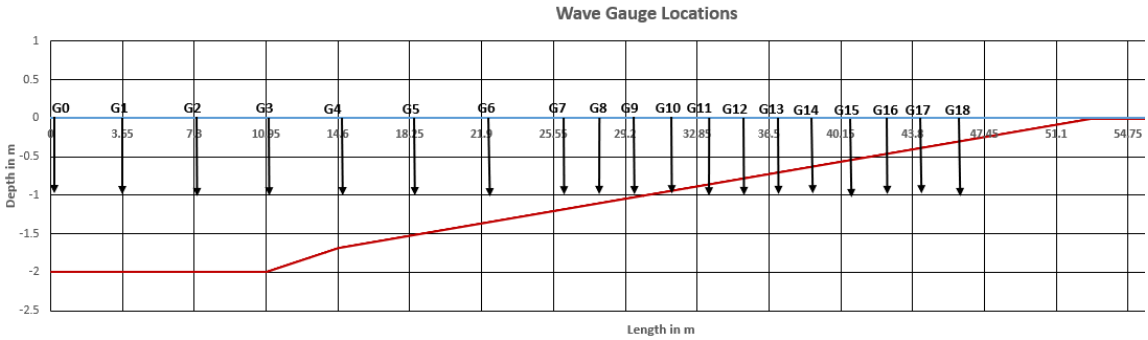

Figure 6: Gauge (0-18) locations with basin profile in models.

Experimental data consists of waves run at time periods 6, 7, and 8 seconds with Cnoidal and Random waves and their combination. Test combinations consisted of Cnoidal only, 3 random waves, and 3 combined waves. Combined waves data is as follows

T (s)	Cnoidal H (m)	Random Hs (m)
6	0.49	0.89
6	0.71	0.71
6	0.89	0.49
7	0.49	0.89
7	0.71	0.71
7	0.89	0.49
8	0.49	0.89
8	0.71	0.71
8	0.89	0.49

Table 3: Wave height details of each case.

Each period that is has seven trials first one is pure cnoidal second through fourth pure random and fifth through seventh combined cnoidal and random waves. The input data that is the time series of input wave is measured at the self-calibrating wave gauge and in models we consider that as the zero X coordinate. Total sampling time for the all

the second through seventh trials was same that is around 1200 seconds that is 20 min and all the first trials were same and around 620 seconds that is about 10 min. Time step for the sampling was fiftieth of a second, so the number of samples are as per the time of sampling.

3.3 Models and Setup

Matlab® is being used in the modeling and simulation. Some internal functions are used in the models like fast Fourier transformation (fft), inverse Fourier transformation (ifft) and Hilbert transformation (hilbert). Used Runge-Kutta formulation to model state at next step as an explicit function of the current value of the state and its derivatives. The step implies the millimeter resolution.

In the models the minimum water depth h is set to be one centimeter. Time step is set to be equal to the time step in experiments. X direction step is set to be one millimeter for better accuracy. Water density is set to be 1025 kg/cu.m. ‘b’ is set to be 1.2 and gamma is set to be 0.6 which are parameters in the Thornton and Guza dissipation theory which defines ratio of front face covered in white water (normally $0.8 < b < 1.7$) and defines the ratio of Hrms and h in the saturated surface ($0.4 < \text{gamma} < 0.8$) respectively.

Each first trial data is divided into 15 individual realizations of 2048 data points to have a wave with time-period around 40.96 sec. Similarly, second through seventh trials were divided into 29 individual realizations of 2048 data points which gives a wave with time-period 40.96 sec. An example plot of output from wave gauges 4 to 6 is given below.

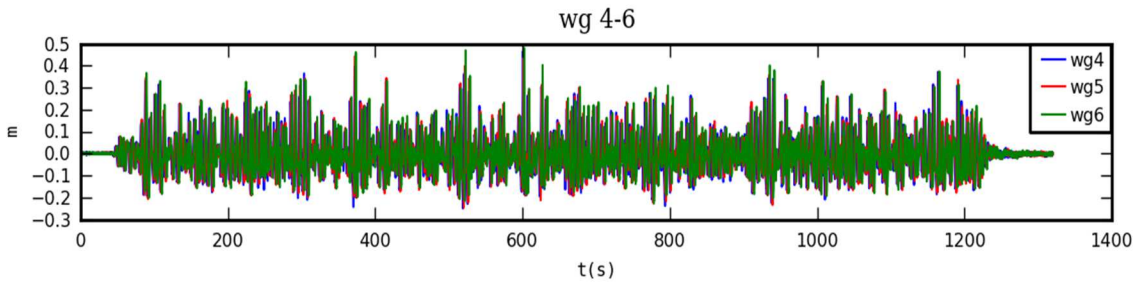

Figure 7: Wave gauge output example.

Initial data till 720 data points were ignored because the wavemaker takes some time to give the required wave. And likewise, data at the end of the output is also vomited to have better accuracy. Fast Fourier transform (fft) function in Matlab is used to calculate the complex amplitudes of the wave and the respective phase. As we get the out put of fft in both positive and negative side of the frequency bands we double the amplitudes and use only one side of the spectrum and that's on the positive side. Each doubled complex amplitude is associated with frequency (Hz) steps and the quantity of the step is calculated from the time step used in the experiments.

Wave number is always calculated using the linear dispersion relation that is equation (2.16). So, Newton-Raphson method is used to iterate the wave number value with input of wave number (which change for every equation) and water depth at that x direction step. With these as the input the models are run to have the complex amplitudes at every gauge location for comparison and saved. With these amplitudes spectral density is calculated and associated with respective frequency. We are only interested in the spectrum till the frequency is thrice the peak frequency because the rest of the data is normally of little to no interest to us.

The evolutionary characteristics of the waves are parametrized using the Asymptotic behavior studies. Skewness and Asymmetry are calculated using the water surface elevation at required distance from the wave maker using inverse fast fourier transform (ifft) function in the Matalb.

$$Skewness = \frac{\langle \eta^3 \rangle}{\langle \eta^2 \rangle^{3/2}} \tag{3.1}$$

$$Asymmetry = \frac{\langle H(\eta)^3 \rangle}{\langle \eta^2 \rangle^{3/2}} \tag{3.2}$$

where H denotes the Hilbert transform and Hilbert transform function in Matlab is used for this purpose in the models and '< >' brackets resemble ensemble average. Skewness and Asymmetry are statistical third moments that represent wave shape at that location and its evolution.

4. MODEL RESULTS AND COMPARISON

4.1 Spectrum comparison

At each wave gauge location, the complex amplitudes solved are saved in the workspace of the Matlab. Spectral energy has been calculated for all the realizations and averaged for a single output spectrum per wave gauge in both models and also for the experimental data. Plots for spectrum are always scaled in log scale for Y axis that is the spectral energy and X axis in this study represents ratio of frequency and calculated peak frequency. Reason for the above approach is to have a better look of Infra, Swell, and Sea regions in the spectrum. Very less plots can be included in this section but most of the plots are included in the appendix section of the thesis.

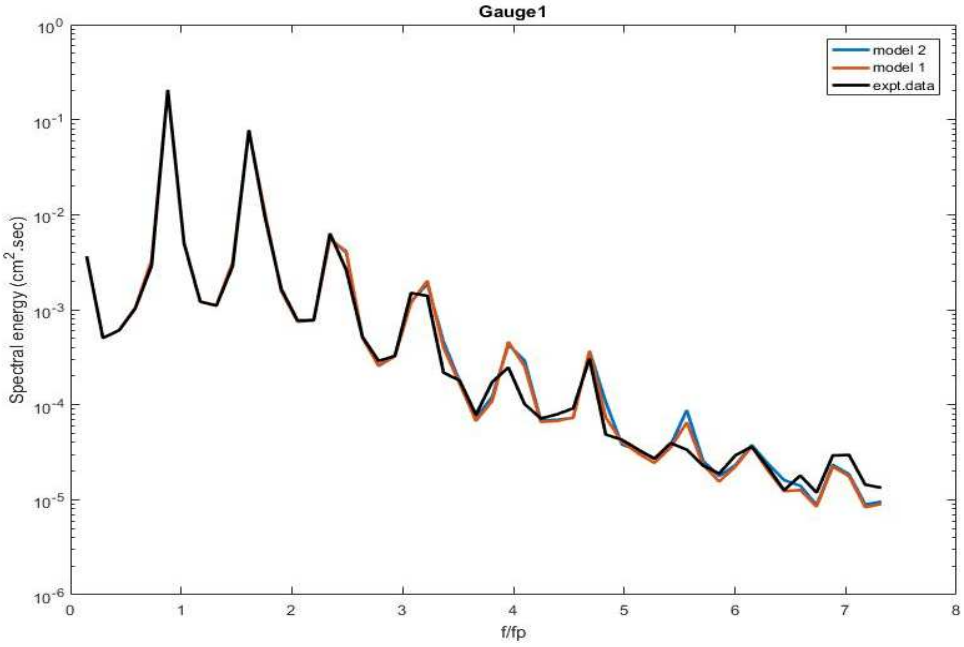

Figure 8: Gauge one, comparison of M1, M2 and Expt. of pure cnoidal wave case.

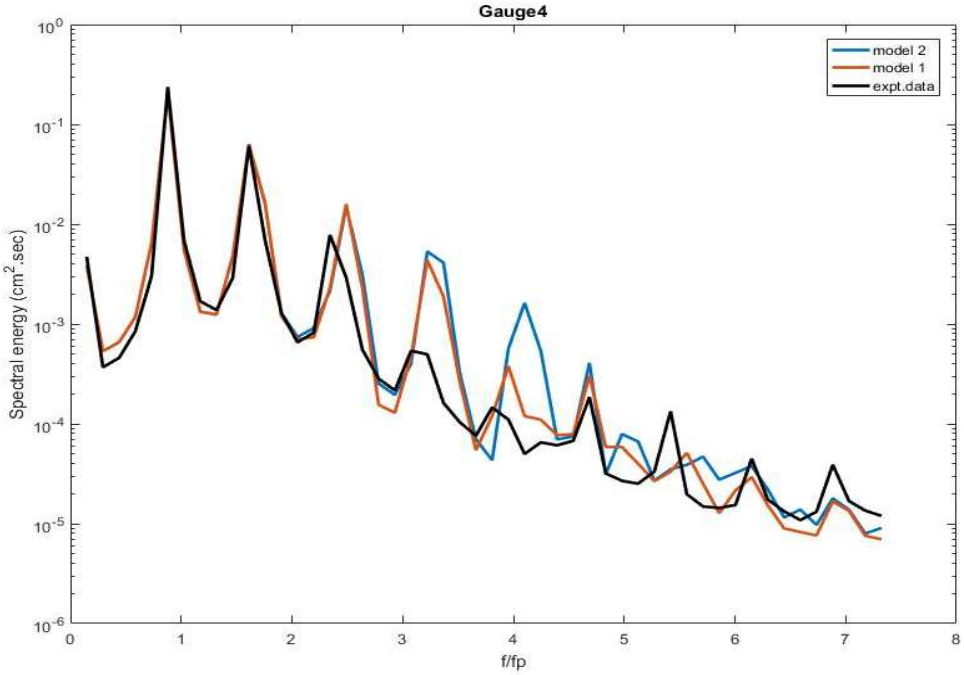

Figure 9: Gauge four, comparison of M1, M2 and Expt. of pure cnoidal wave case.

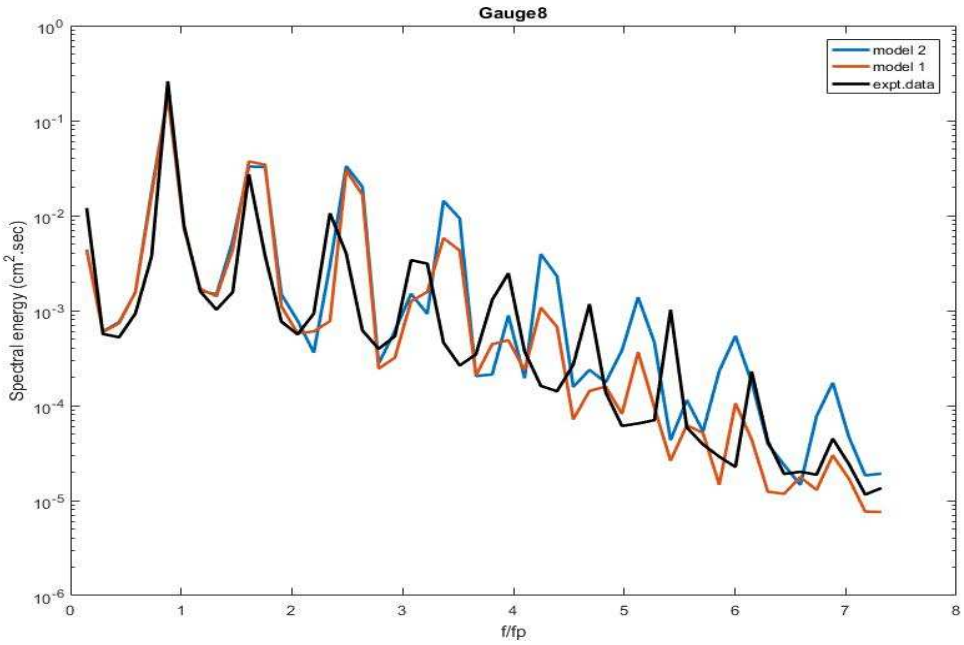

Figure 10: Gauge eight, comparison of M1, M2 and Expt. of pure cnoidal wave case.

Selection of the three gauges 1, 4, and 8 was important because they are on different slopes in both the models and experiment that are 0, 1/12, and 1/24 respectively. As we can observe from the plots the peak of the spectrum is close to 0.97fp in all of the plots in all cases. And model one, that is Mase and Kirby equation based is in better proximity of the experimental data than that of the model two that is fully dispersive nonlinear model. We will discuss the inference after the pure random and combination of random and cnoidal cases are observed. The trial cases are from the waves with time period 8 sec. We can also see the gradual separation of accuracy in the models from gauge one to gauge eight.

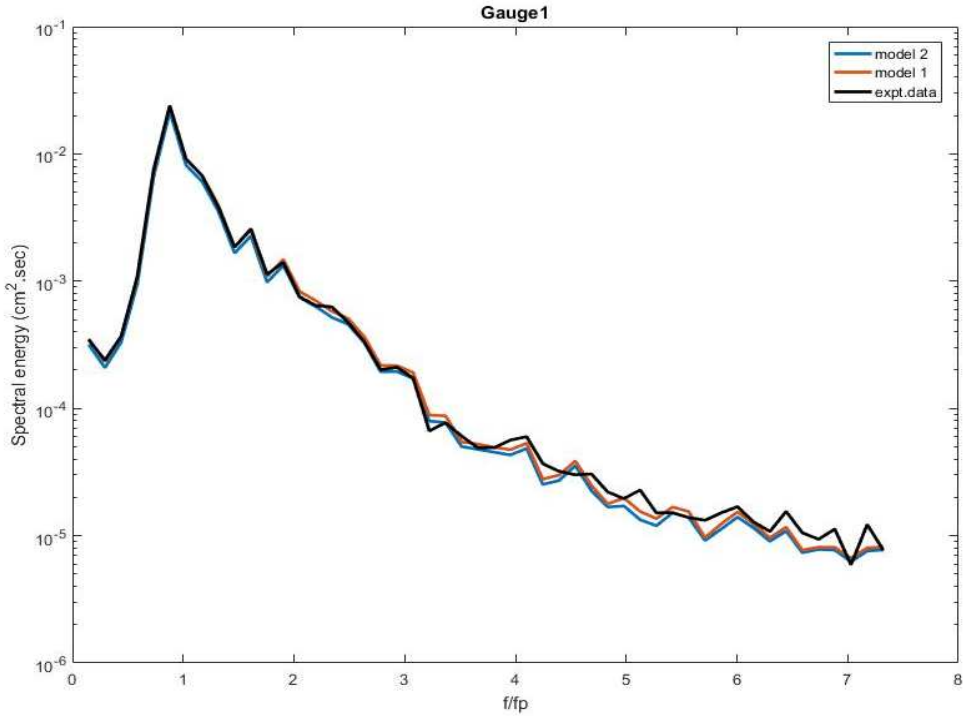

Figure 11: Gauge one, comparison of M1, M2 and Expt. of just random wave case.

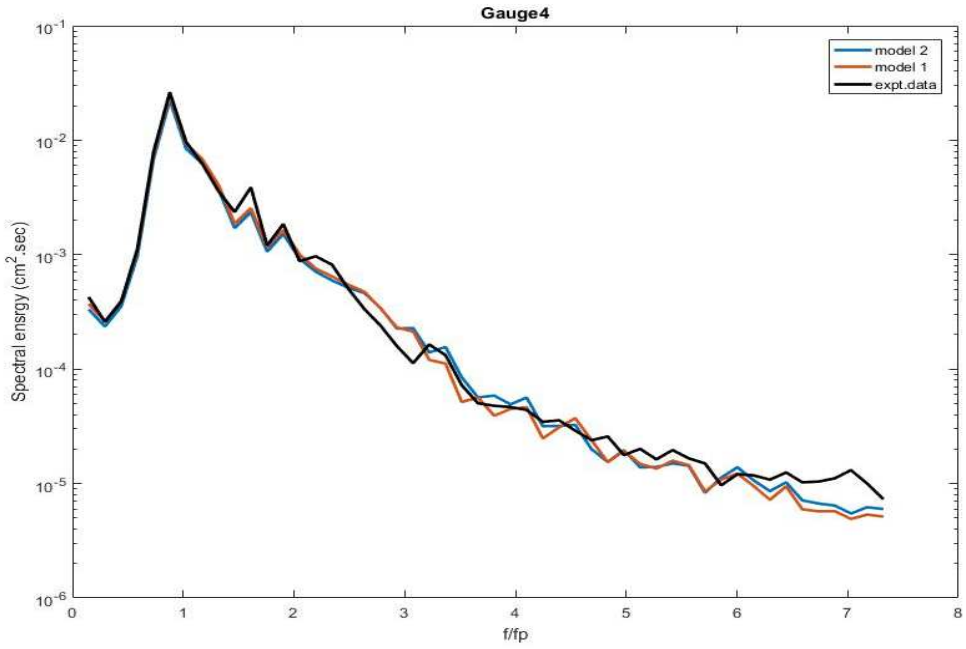

Figure 12: Gauge four, comparison of M1, M2 and Expt. of just random wave case.

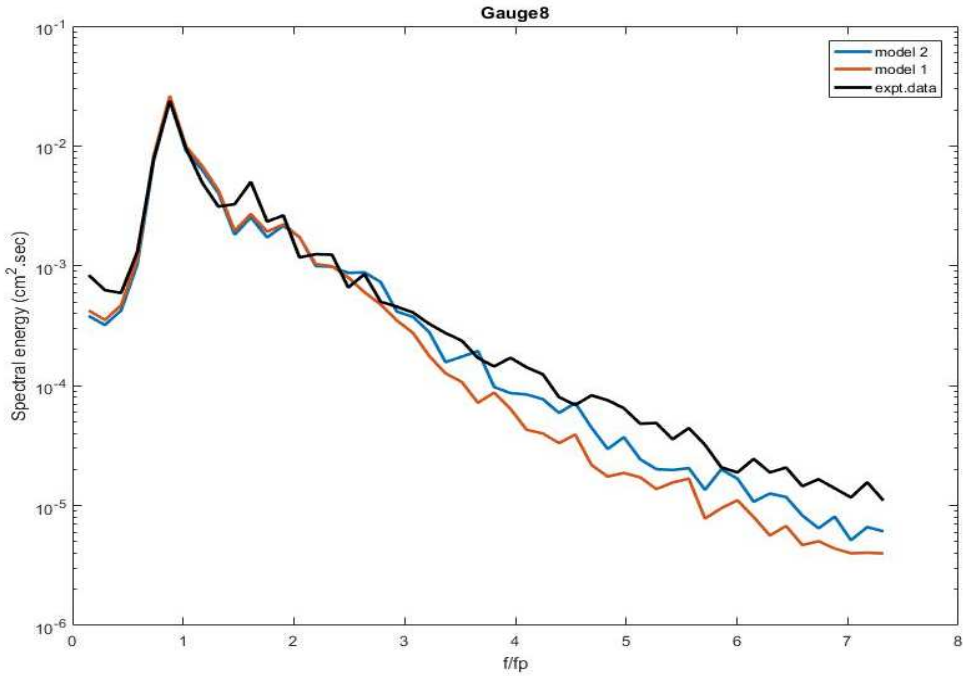

Figure 13: Gauge eight, comparison of M1, M2 and Expt. of just random wave case.

And model two that is fully dispersive nonlinear model is in better proximity of the experimental data than that of the model one, that is Mase and Kirby equation based. We will discuss the inference after the combination of random and cnoidal cases are observed.

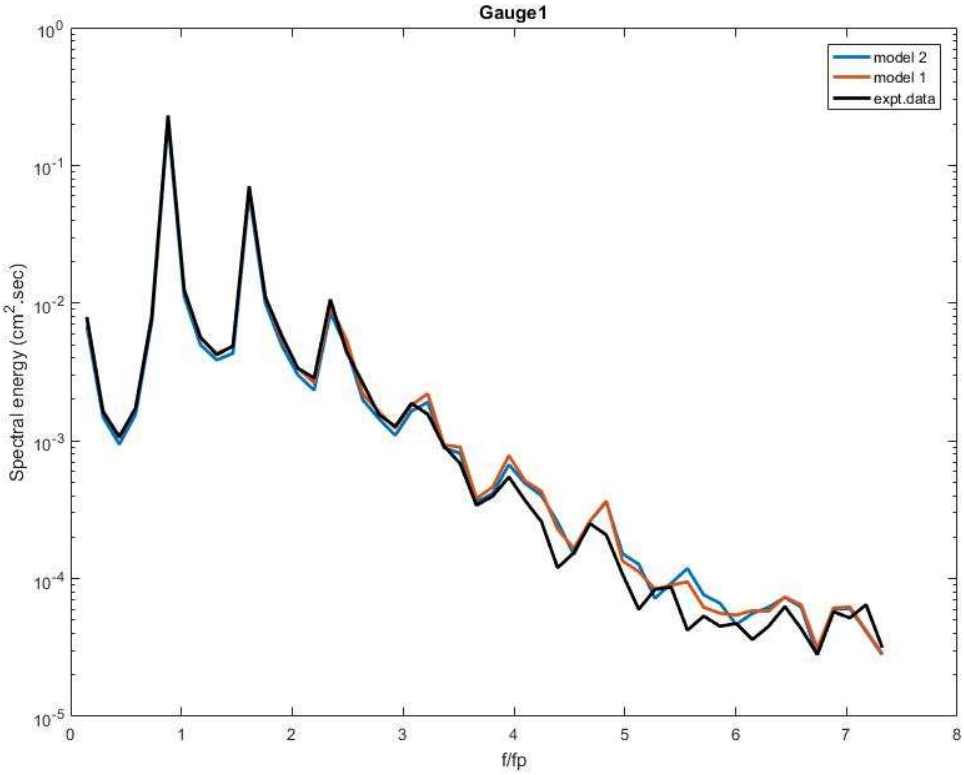

Figure 14: Gauge one, comparison of M1, M2 and Expt. of random and cnoidal wave case.

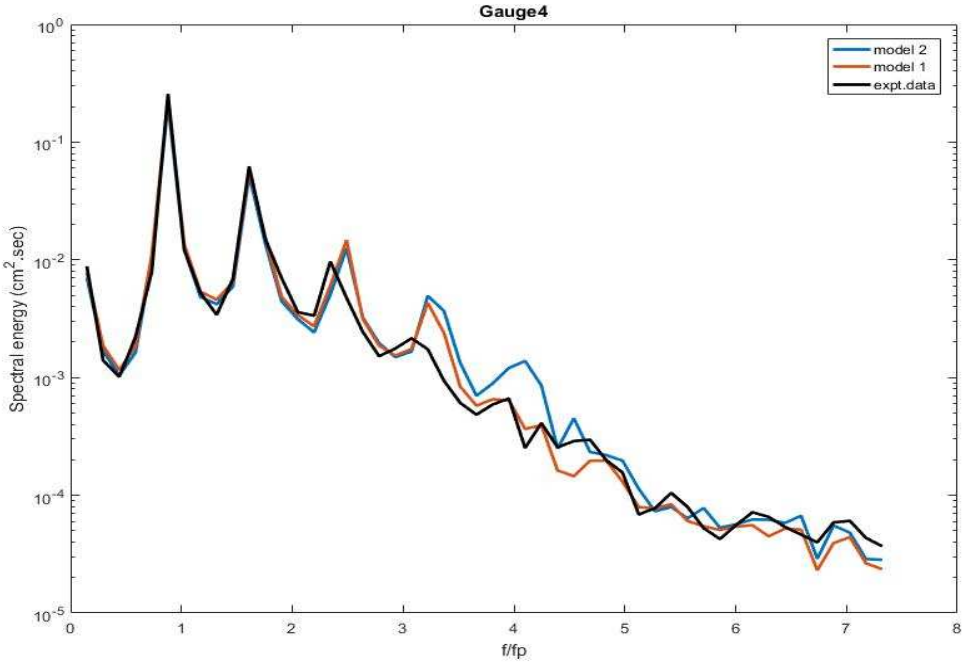

Figure 15: Gauge 4, comparison of M1, M2 and Expt. of random and cnoidal wave case.

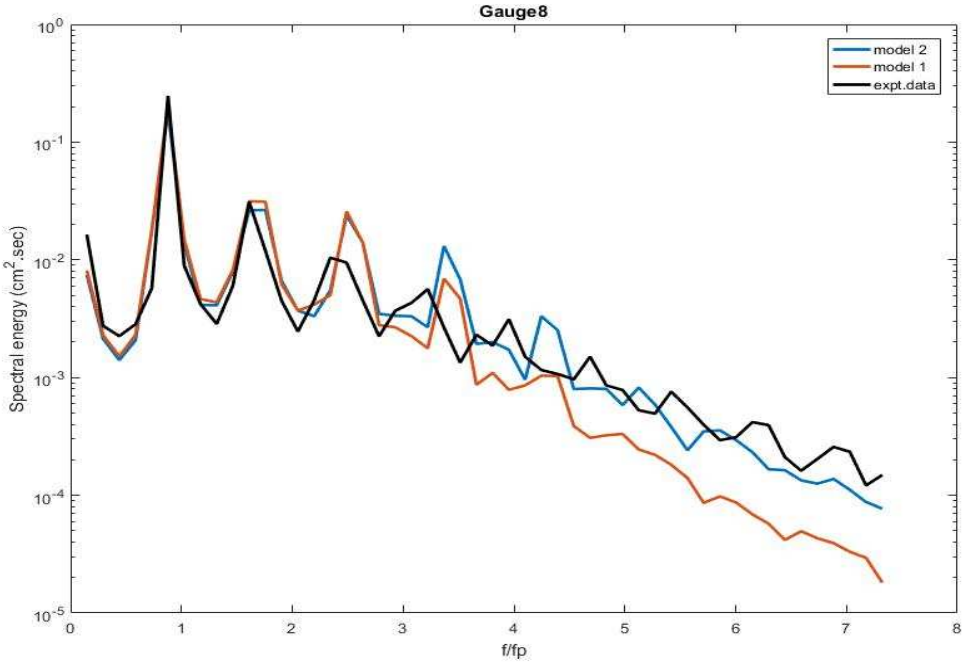

Figure 16: Gauge 8, comparison of M1,M2 and Expt. of random and cnoidal wave case.

And model two, that is fully dispersive nonlinear model is in better proximity of the experimental data than that of the model one, that is Mase and Kirby equation based. Same wave trial cases are examined for the time periods 6 sec and 7 sec and the observed results are as following.

	6 Sec Time period	
Trial 1	Trial 2	Trial 5
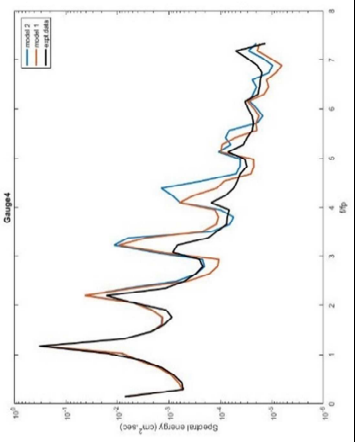	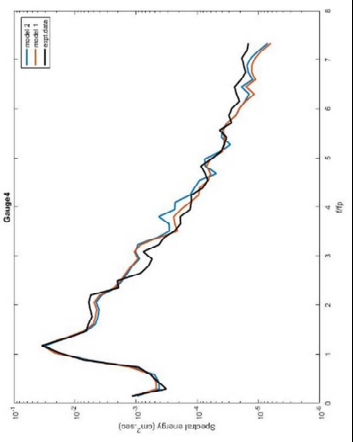	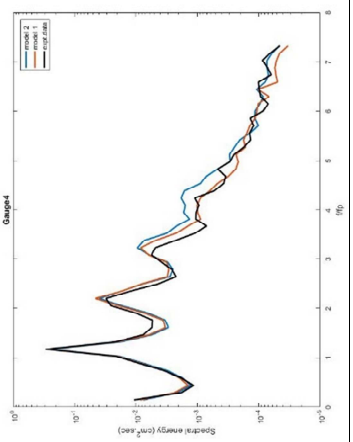
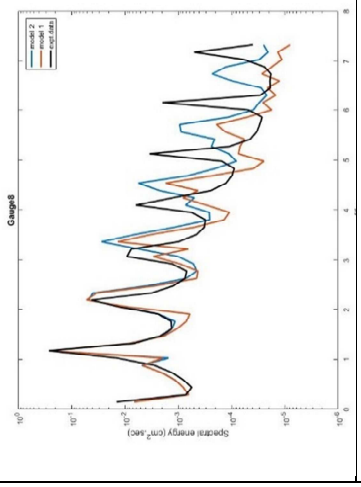	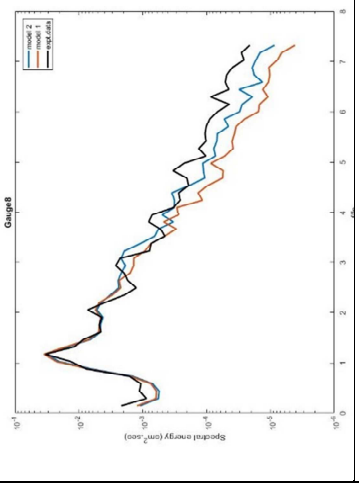	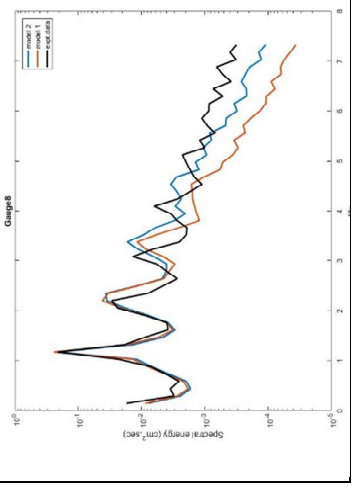

Table 4: 6 sec time period wave spectrum Trials 1,2 and 5 and their gauges 4 and 8

	7 Sec Time period	
Trial 1	Trial 2	Trial 5
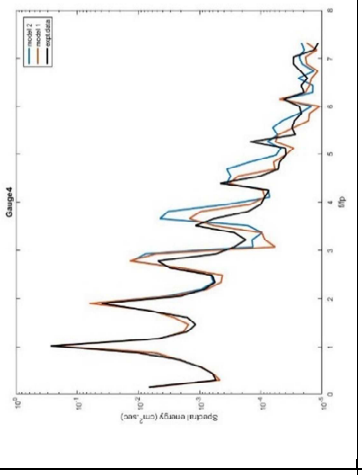	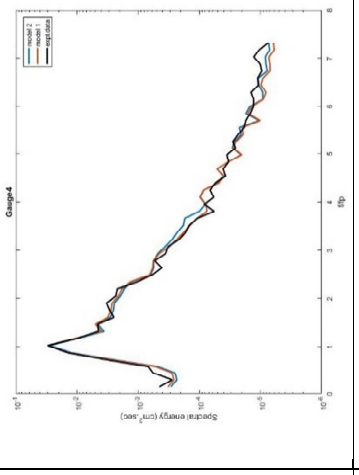	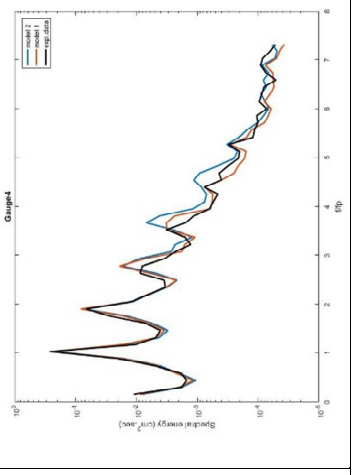
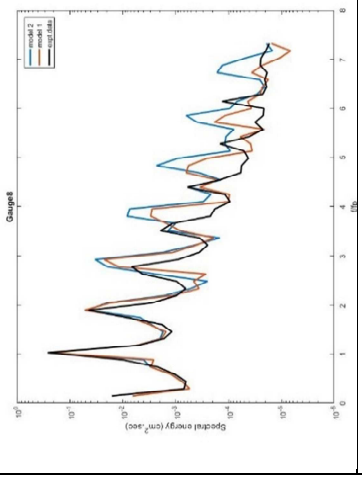	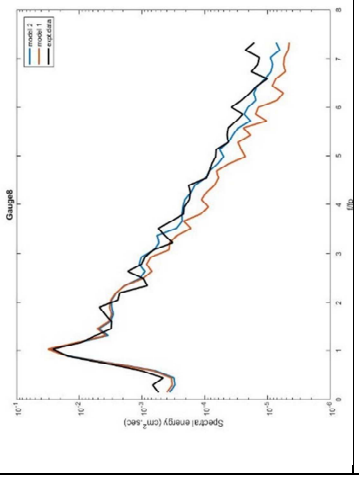	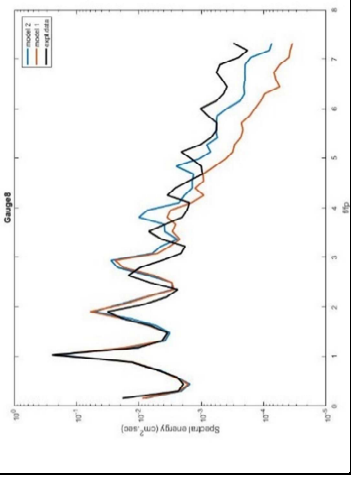

Table 5: 7 sec time period wave spectrum Trials 1,2 and 5 and their gauges 4 and 8

4.2 Third moments and Hrms.

From all the above plots we can observe that the model one does better in the pure cnoidal wave trials and model two does better in the just random and combined cnoidal and random trials. Ursell number of the cnoidal waves is very high and so prediction of these waves is good with shallow water approximated equations-based models.

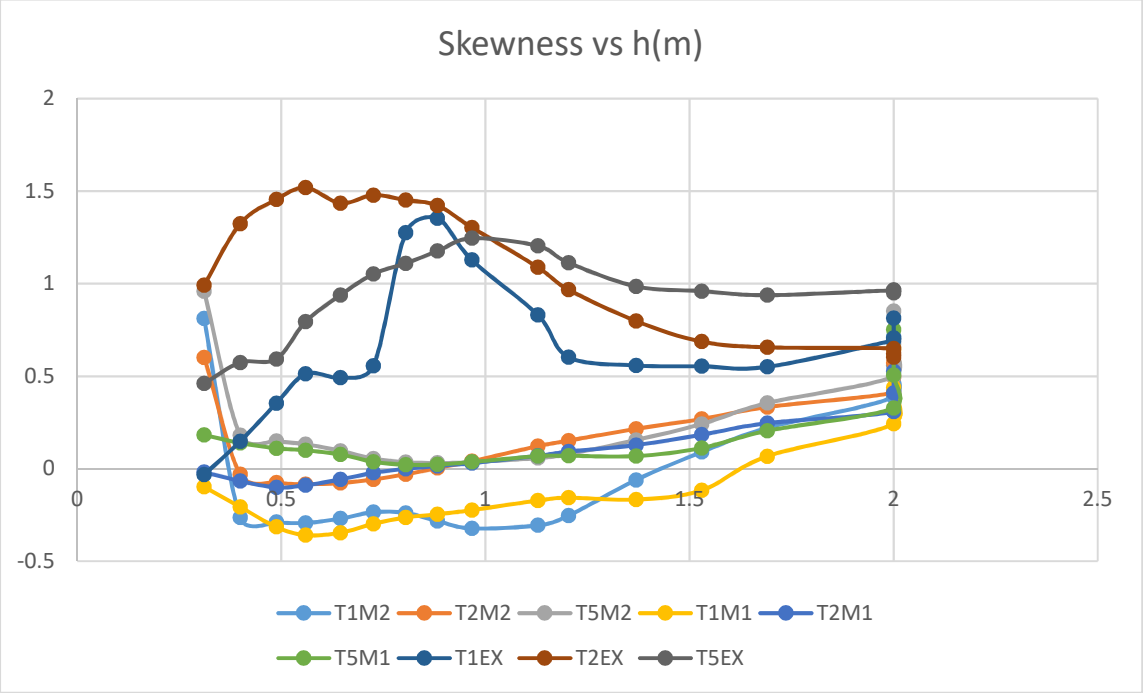

Figure 17: Skewness Vs h(m) plot for Trials 1,2, and 5 for both models and experiment.

Skewness trend with respect to water depth for trial 1 in M1 and M2 along with trial 5 in M1 and M2 seems to be out of trend with rest of the trials and mainly experimental data.

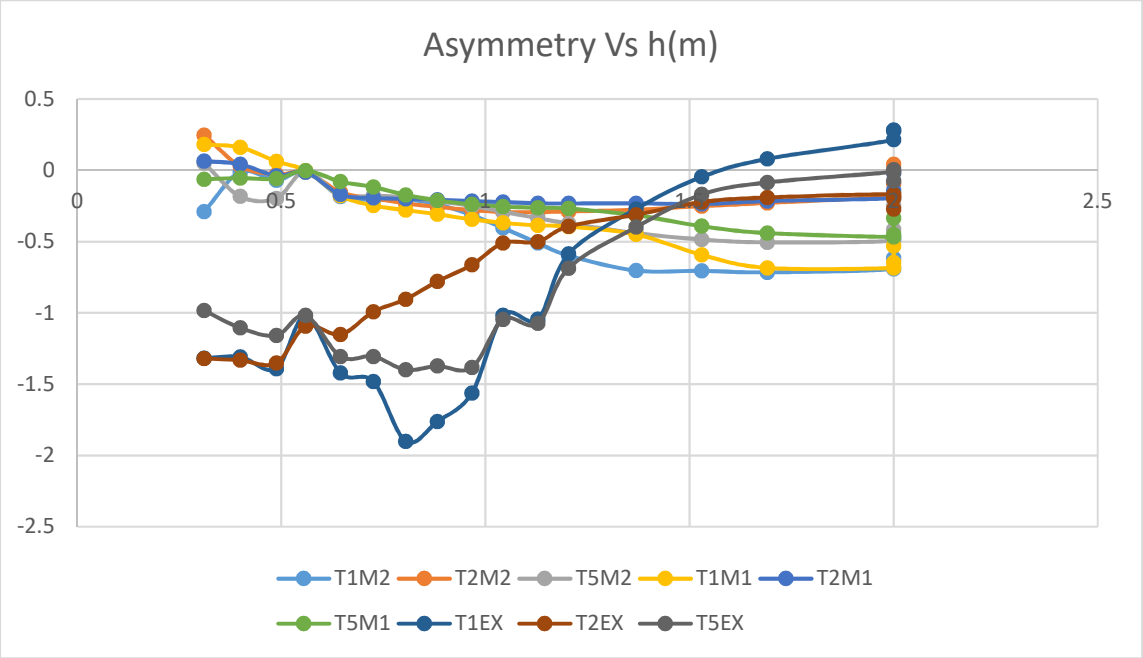

Figure 18: Asymmetry vs h(m) plot Trials 1,2, and 5 for both models and experiment.

As expected asymmetry values are negative in almost all the gauges location. Trial 1, 2 and 5 of experimental data seems to follow a different trend than that of the rest trials.

Area under the spectral energy vs frequency plots is calculated and plotted comparing M1, M2, and Experimental data with each other in three regions of the spectra namely Infra gravity wave region, Swell wave region, and Sea wave region. We divided the regions based on the peak frequency of the spectrum. First Infra gravity region is selected as the frequency region from first frequency step to half of peak frequency. Second the swell wave region of spectra is selected starting from half of the peak frequency to three times half of peak frequency and the rest is considered in the sea wave region till three times the peak frequency.

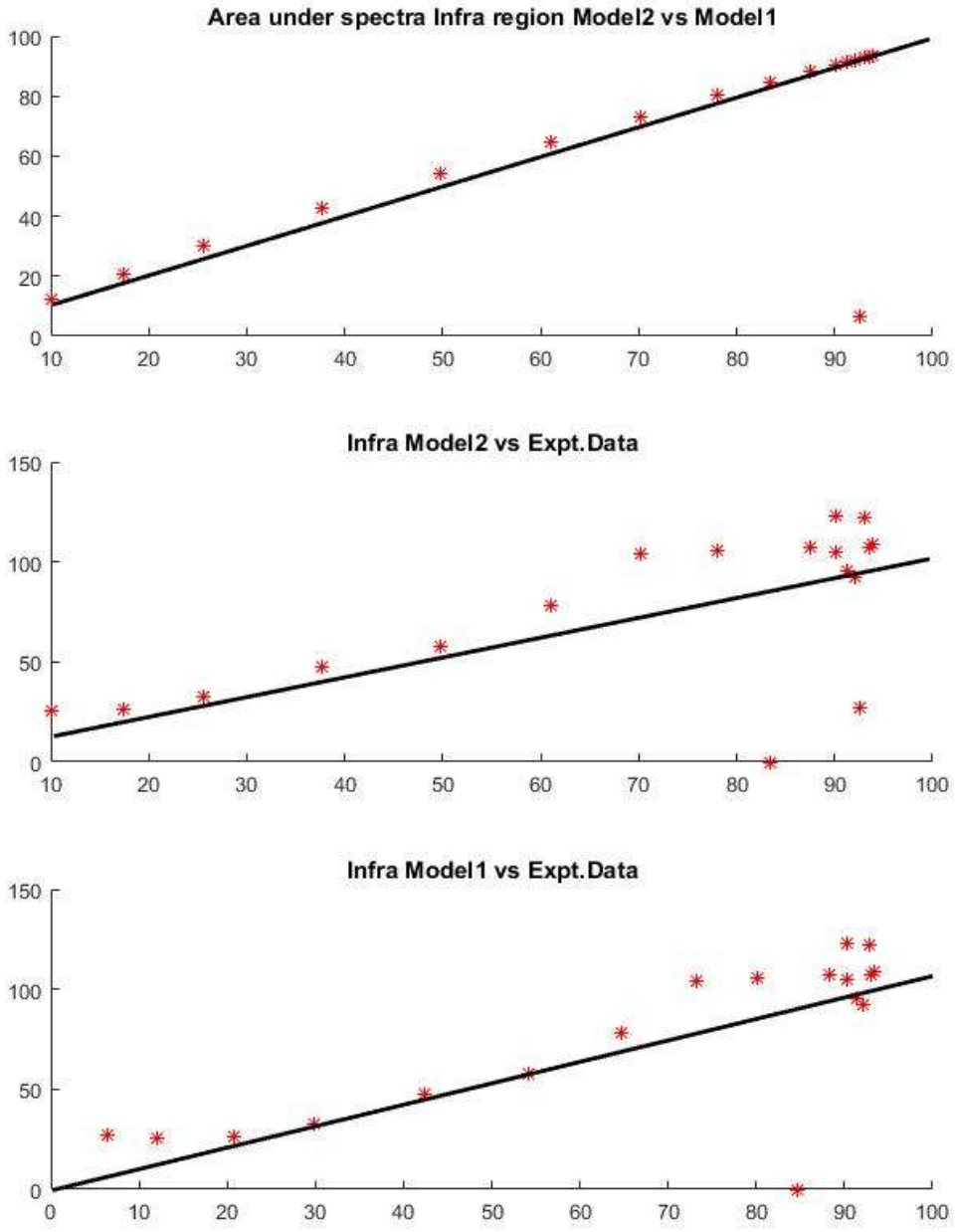

Figure 19: Area under spectra for trials 1,2, & 5 in Infra gravity wave region and reference x=y.

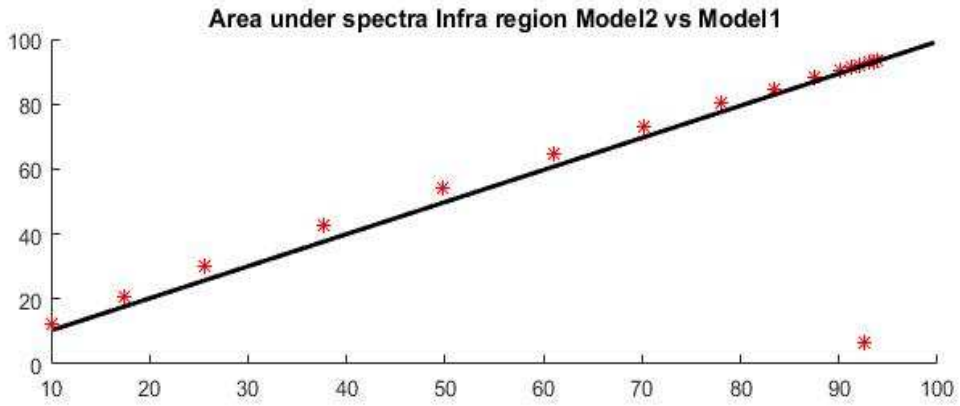

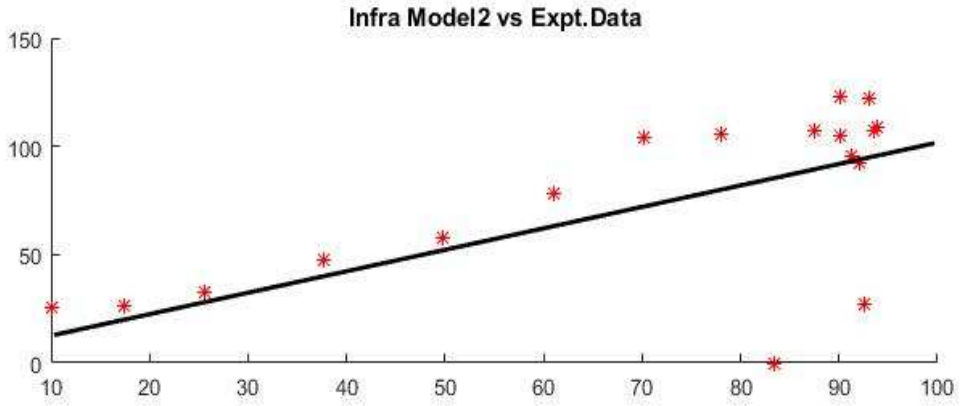

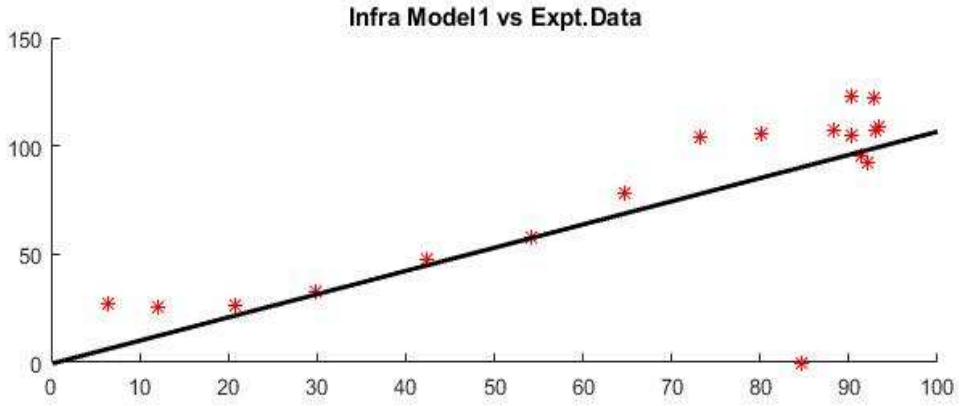

Figure 19: Continued.

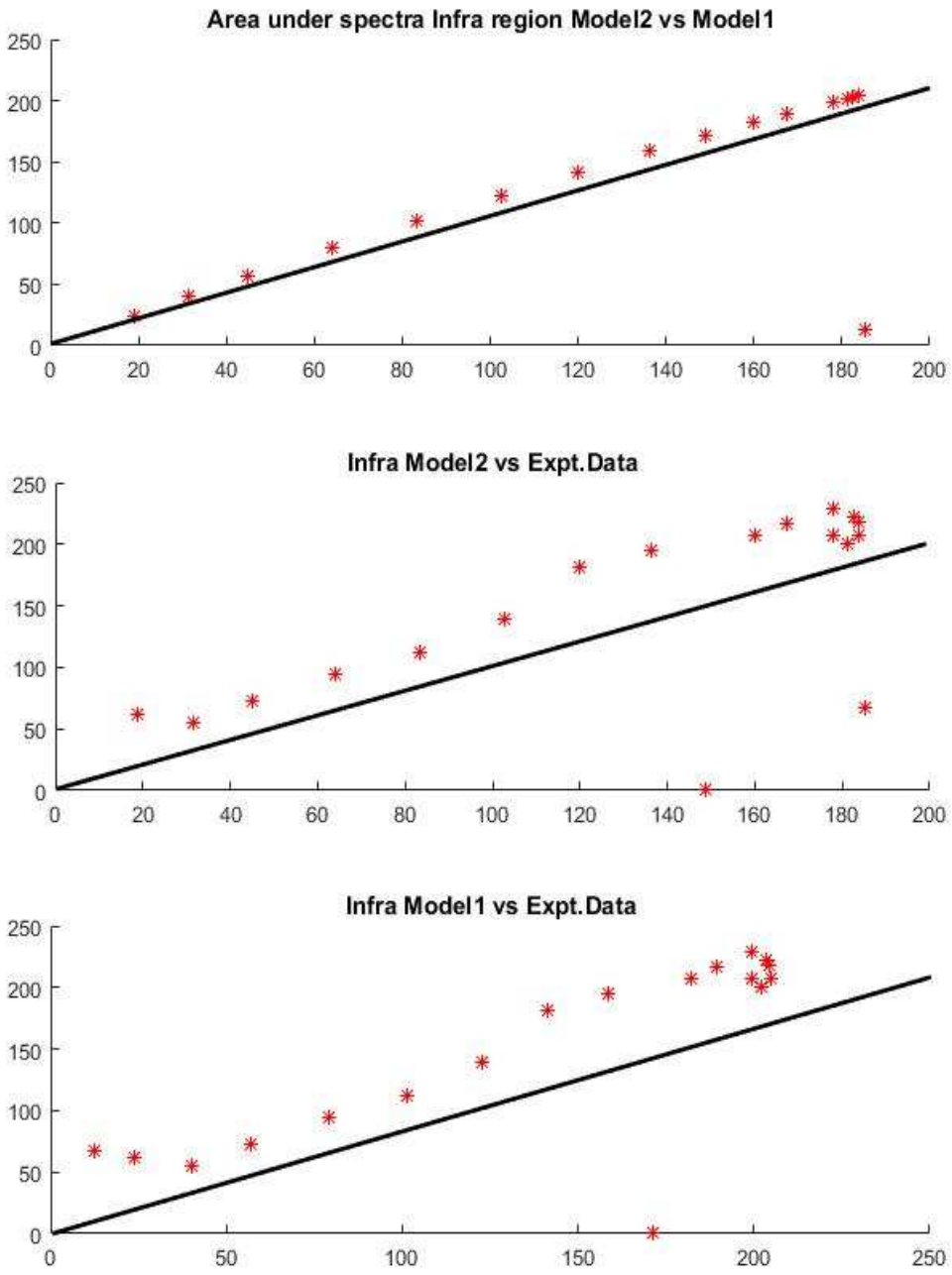

Figure 19: Continued.

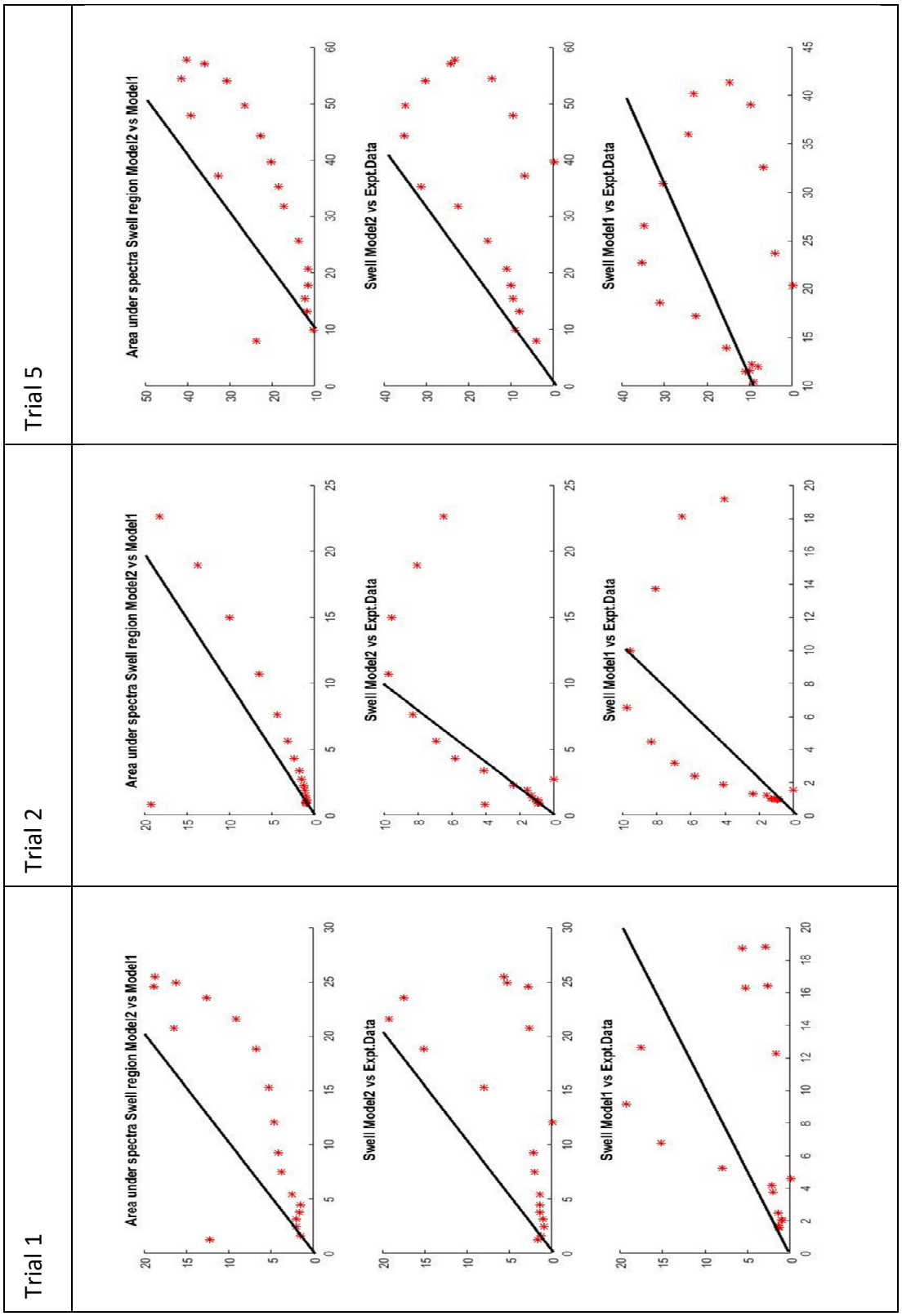

Table 6: Area under spectra for trials 1, 2, and 5 in Swell wave region.

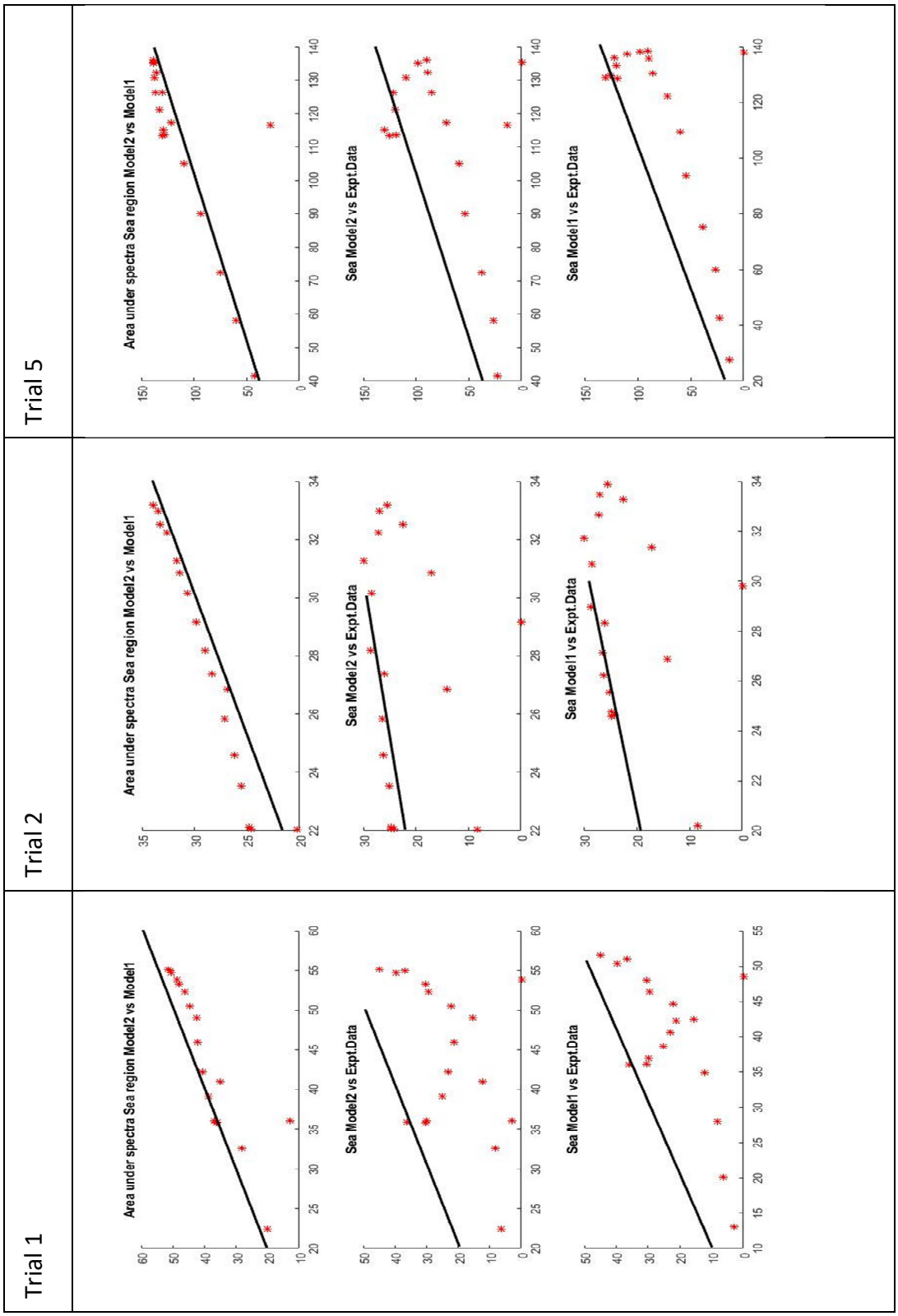

Table 7: Area under spectra for trials 1, 2, and 5 in Sea wave region.

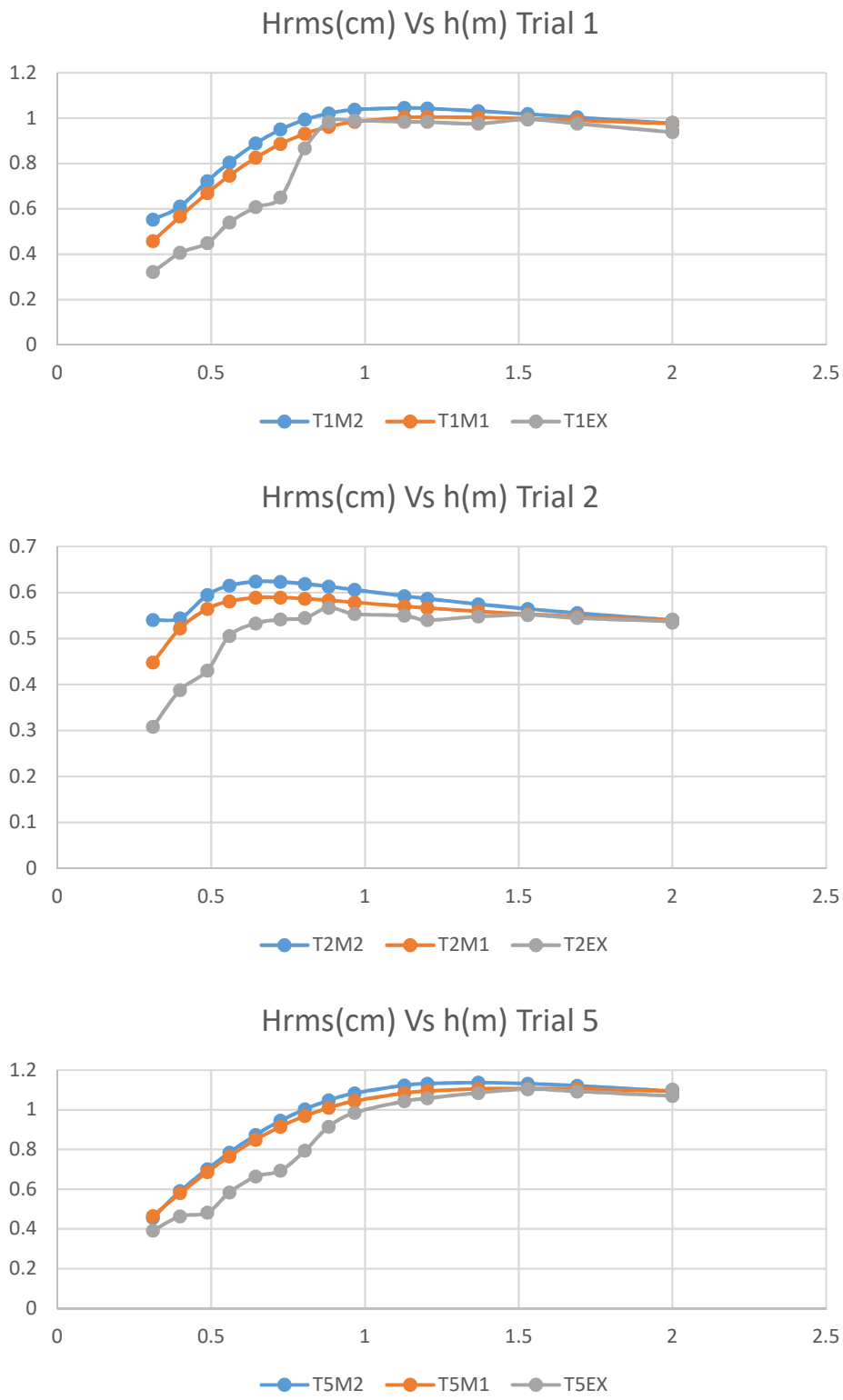

Figure 20: Hrms Vs h plots of three trials from seven second wave period case.

5. INFERENCE AND SUMMARY

As mentioned earlier the study is to compare two different models to the experimental data from the OSU lab and to find the condition under which the models do a better prediction of wave transformation while going towards shore. The models are based on equations 2.22 and 2.24. Both models have same degree of nonlinearity, and the dispersion relation is completely linear in model one and approximated to second order nonlinearity in model two. The dissipation terms are same in both of the models and work the same irrespective of the dissipation properties.

In this section we discuss the inference of the data and comparison plots shown in the section 4. We observed that the fully dispersive nonlinear model that is model one is doing good in predicting the wave data that is purely cnoidal and the weakly dispersive nonlinear model that is model two with same dissipation terms as model one is doing better in predicting the just random and combined random and cnoidal wave case. If we take the natural occurrence in to consideration either waves are random or in rare cases the cnoidal waves combine with random and occur in the time of tsunamis. So, we can say that the weakly dispersive model that is fully nonlinear is doing a better job in predicting the natural case.

Going into details of the spectrum produced by the models in trial one that is pure cnoidal wave case the spectrum at peak frequency match perfectly. The area under the graph for the infra gravity wave region matches almost perfectly. Crossing the peak frequency, the spectrum produced from model output tends to move out of sync with the

data from experiments. The starting from the third mode spectrum tend to over predict the energy and local peaks tend to move further than the supposed frequencies. Intermediate frequencies are between the multiples of peak frequency acquired energy cause of the nonlinearity nature in the models and are seen clearly in the spectrum plots which is not observed in the experimental data.

Area under the spectrum calculated frequency region wise shows a better picture of the prediction. In Infra gravity wave region the area under the models and data are close and follow a trend to be in and around the x = y line. In the Swell wave region same trend is followed though the plots don't meet in perfect sync the area under the plots seems to be close. The sea wave region of the spectrum shows different trend and the model one is always seen to be under predicting than that of the model two. In the case of pure cnoidal wave the model one is close to the data.

The cases of just random wave and combined random and cnoidal wave seems to follow a similar trend and model two is doing a better job in predicting the cases close to the data. In the infra gravity wave region area under plots of models seem to be lower than that of the data. In the Swell wave region, the plots are perfectly matching the data. In the sea wave region of the plots the models seem to under predict the energy and can be seen clearly in the just random wave case gauge 8 comparison plot. And we can clearly see the model two doing better prediction from the combined case higher frequencies.

The model that is nonlinear with weak dispersiveness built into it is doing a better job than that of model one in predicting the transformation of the waves which have the randomness to its nature.

Reasons for the nonlinear dispersion relation to hold better in the random and combined wave cases may be because the incomplete nonlinearity in the equations complementing the incomplete dispersion relation. In the pure cnoidal wave case the bounded wave nature is closely and not completely followed by the data which can be observed in the spectrum peaks. So, the models might not be considering the pure bound case and so the higher and intermediate frequencies are exchanging the energy among themselves.

Model one is clearly the winner in the case of pure cnoidal wave case. So, we can infer from this study that predicting wave transformation is not always done right by any single model. We can also see that the strong dispersion relation tends to make the model under predict the energy in the higher frequency zones.

REFERENCES

1. Kaihatu J. M. Ph.D. (1994) Frequency-Domain models for nonlinear finite depth water wave propagation.
2. Data reference: Kaihatu J. M., Goertz J.T., Ardani S., and Sheremet A., (2017) Nonlinear and dissipative characteristics of a combined random and cnoidal wave field.
3. Kaihatu J. M., and Kirby J. T., Spectral evolution of directional finite amplitude dispersive waves in shallow water. ASCE library Coastal engineering 1992
4. Kirby J.T., Kaihatu J. M., (1996) Structure of frequency domain models for random wave breaking. ASCE library Coastal engineering 1996
5. Kaihatu J. M., Jayaram V., Kacey L. Edwards, James T. Kirby (2007) Asymptotic behavior of frequency and wave number spectra of nearshore shoaling and breaking waves. Journal of Geophysical Research: Oceans/Volume 112
6. Kirby, James T. and Hajime Mase (1992) Hybrid Frequency domain KdV Equation for Random wave transformation. ASCE library Coastal engineering 1992
7. Chen Y., Guza R.T., Elgar S., (1997) Modeling spectra of breaking surface waves in shallow water. Journal of Geophysical Research: Oceans/Volume 102
8. Eldeberky Y., Battjes J.A., (1996) Spectral modeling of wave breaking: Application to Boussinesq equations. Journal of Geophysical Research: Oceans/Volume 101

9. Freilich M.H. and Guza R.T. (1984) Nonlinear effects on shoaling surface gravity waves.
10. Kirby, J.T. (1990) Modeling shoaling directional wave spectra in shallow water. ASCE library Coastal engineering 1990
11. Kirby J.T., Kaihatu J. M. and Mase H. (1992) Shoaling and breaking of random wave trains: Spectral approaches. ASCE library
12. Peregrine D.H. (1967) Long waves on a beach. Jour. Fluid Mechanics, Vol. 27, pp.815-827. Journal of Fluid Mechanics
13. Sheremet A., Kaihatu J. M., (2011) Modeling of nonlinear wave propagation over fringing reefs. Elsevier library Coastal engineering Volume 58 issue 12
14. Edward B. Thornton and R. T. Guza (1983) Transformation of wave height distribution. Journal of Geophysical Research: Oceans/Volume 88 issue C10
15. Kirby, J.T., Kaihatu, James M. (1995) Nonlinear transformation of waves in finite water depth. AIP Physics of fluids Volume 7 issue 8.
16. Figure one reference 2004 Indian ocean tsunami near Koh Pu Island P.C. Anders Garwin
17. Figure 2 and 3 reference OSU official website https://oregonstate.designsafe-ci.org/

APPENDIX

Results from 7 Sec wave period case in trial 1, 2, and 5.

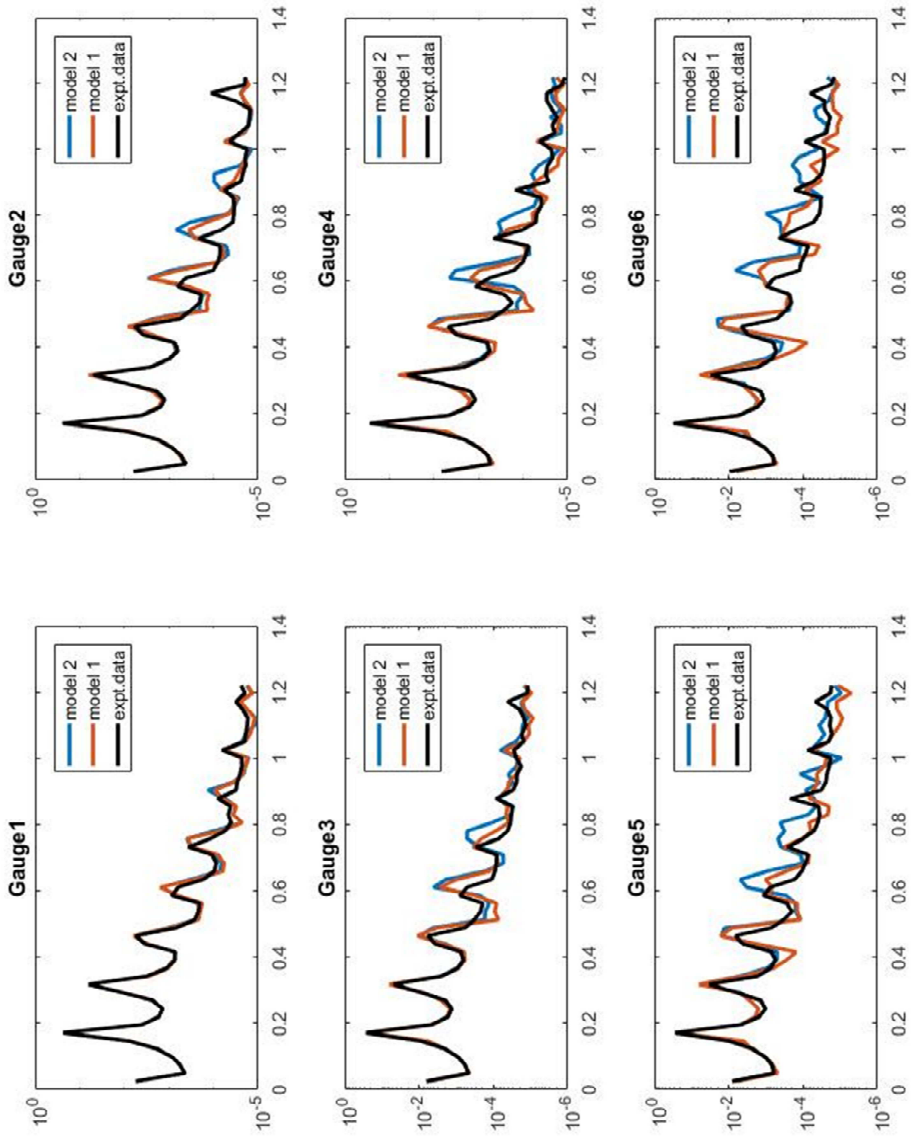

Gauge 1-6 Trial 1 comparison of M1, M2 and Expt. spectral density (cm^2.s) Vs frequency (Hz)

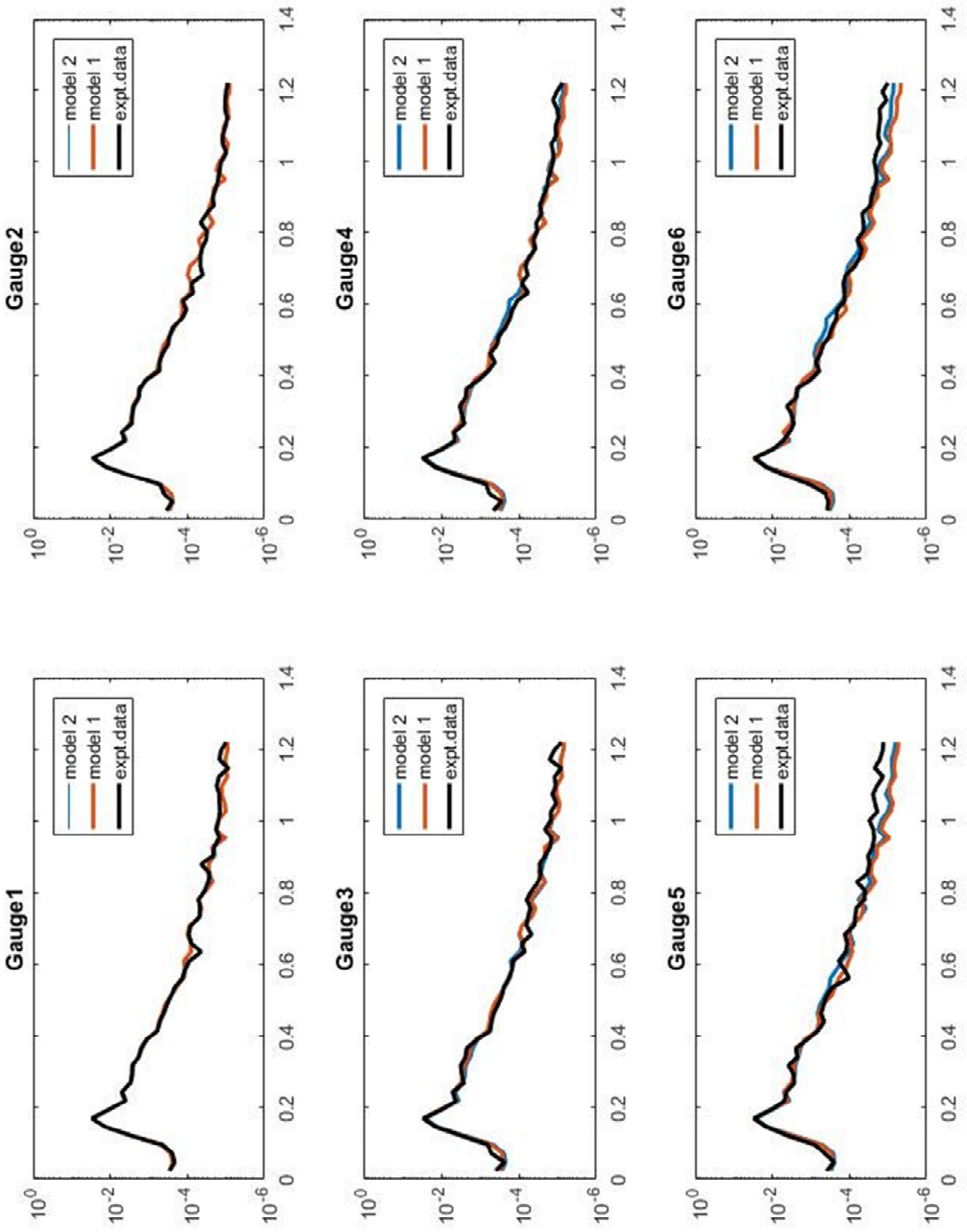

Gauge 1-6 Trial 2 comparison of M1, M2 and Expt. spectral density (cm^2.s) Vs frequency (Hz)

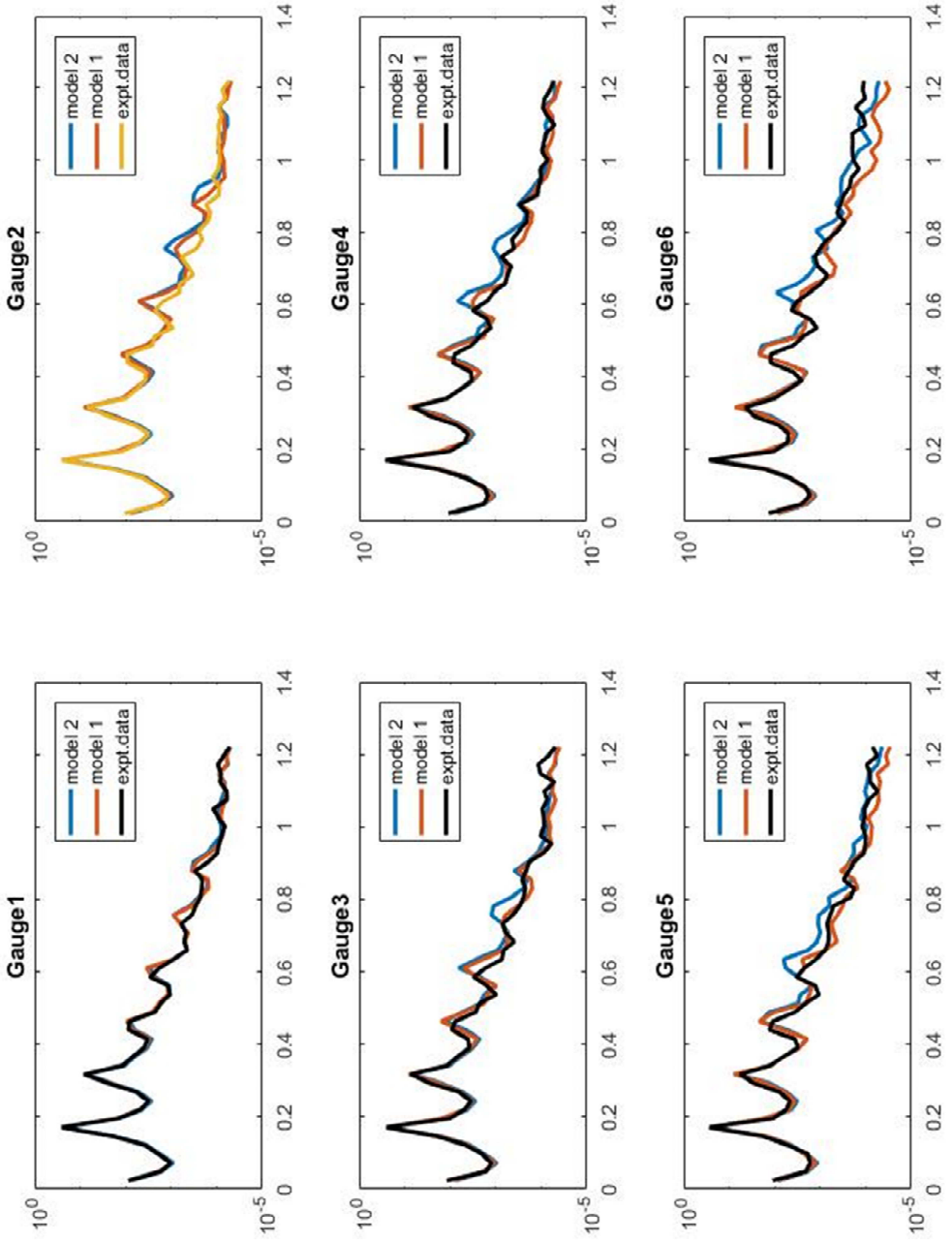

Gauge 1-6 Trial 5 comparison of M1, M2 and Expt. spectral density (cm^2.s) Vs frequency (Hz)

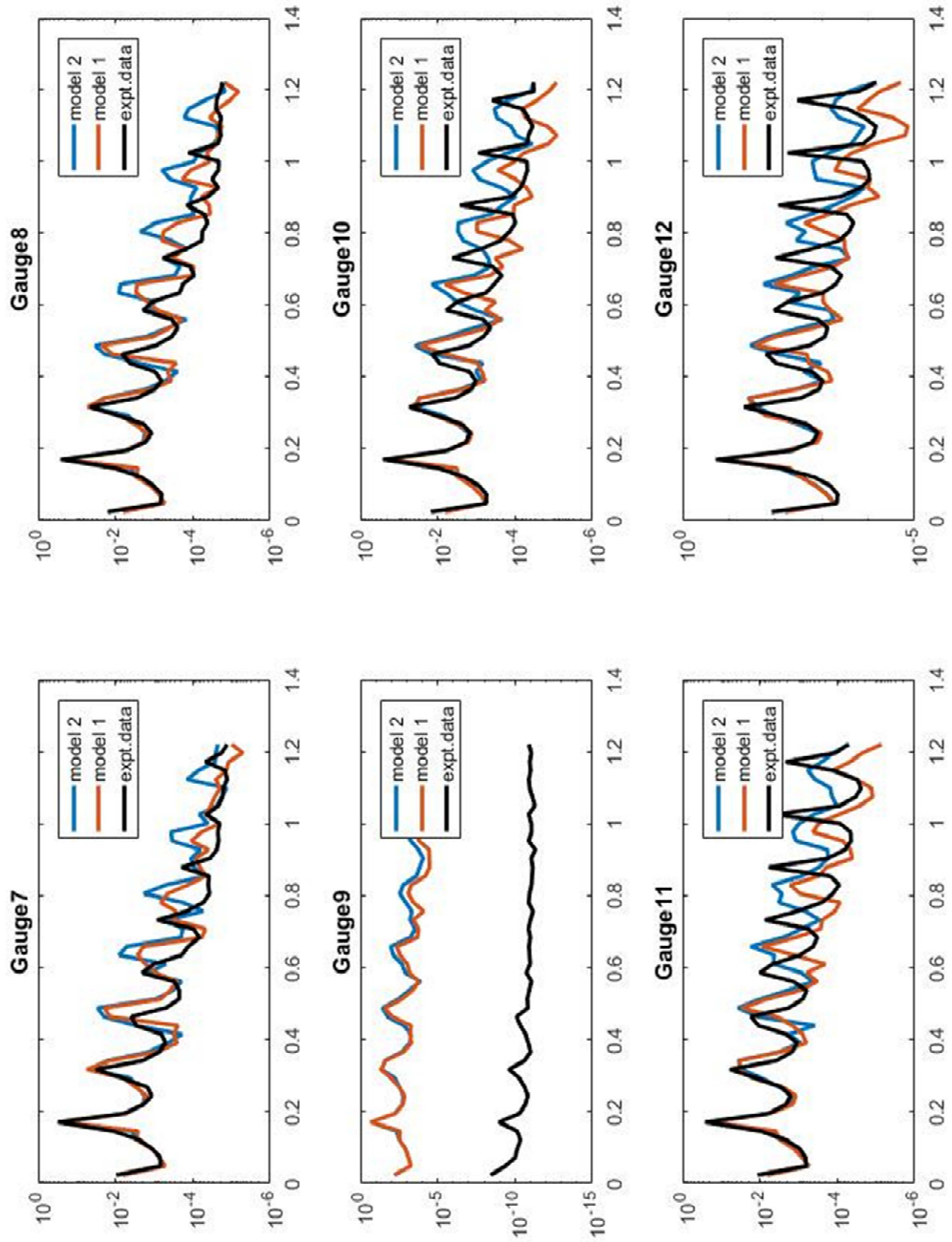

Gauge 7-12 Trial 1 comparison of M1, M2 and Expt. spectral density (cm^2.s) Vs frequency (Hz)

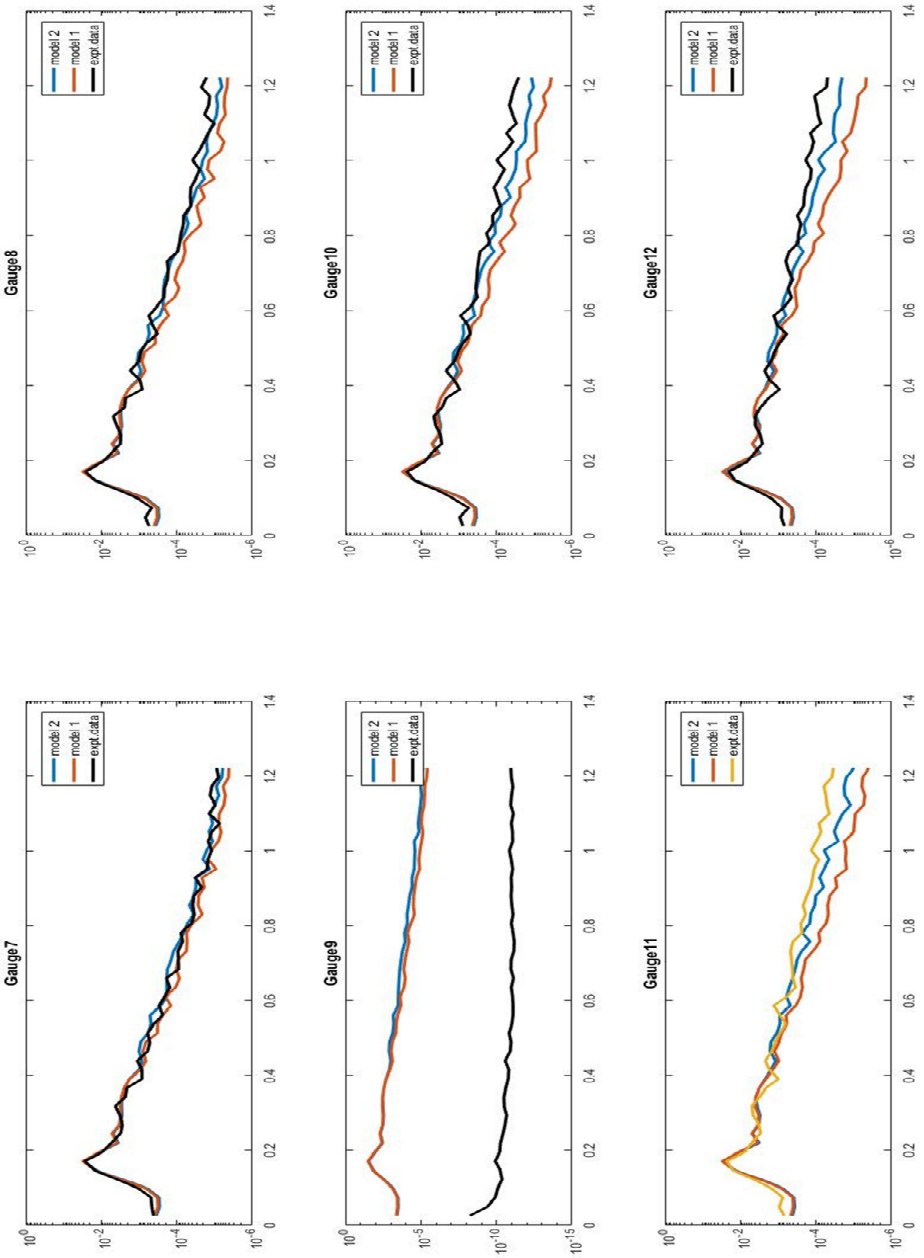

Gauge 7-12 Trial 2 comparison of M1, M2 and Expt. spectral density (cm^2.s) Vs frequency (Hz)

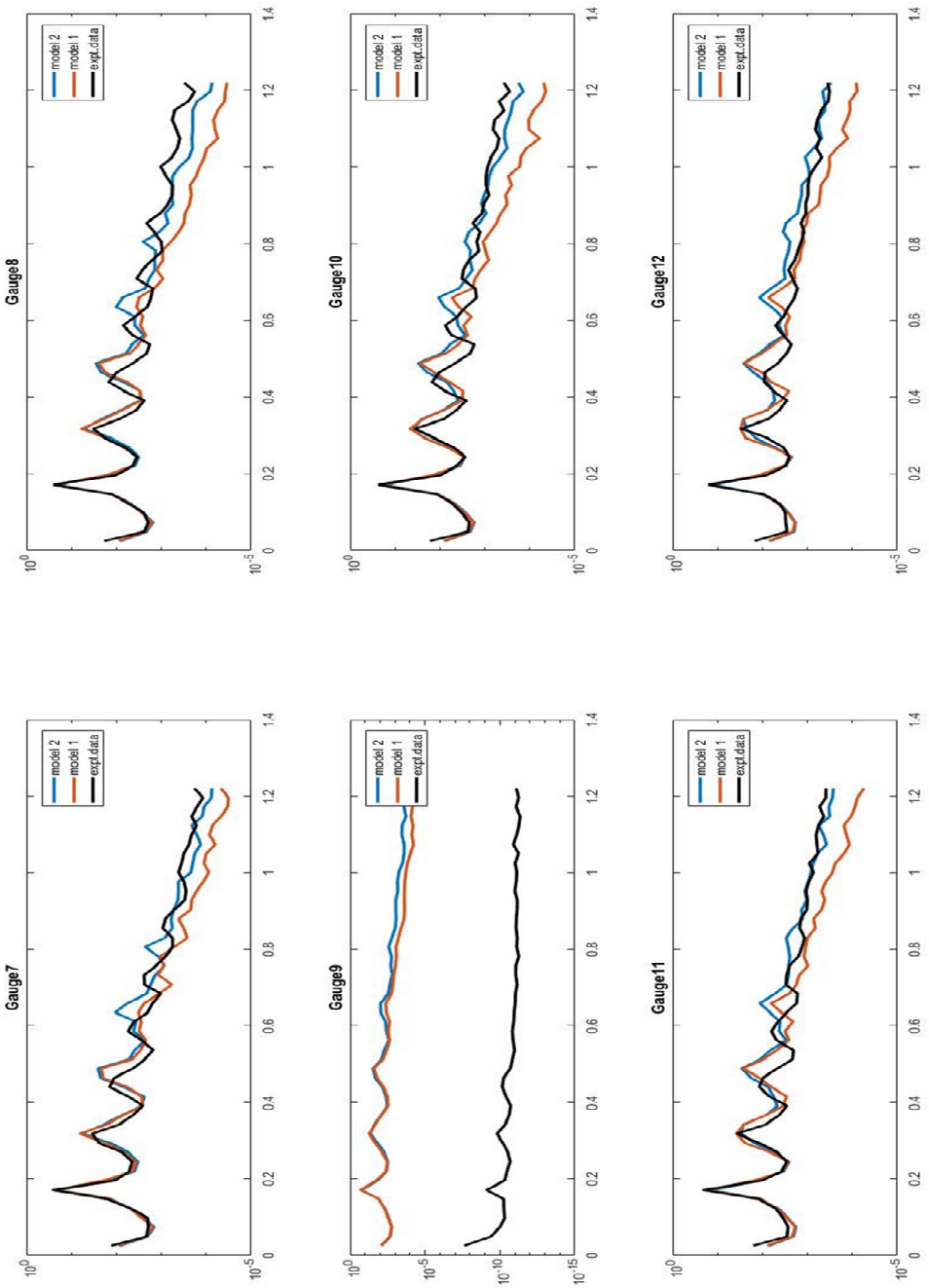

Gauge 7-12 Trial 5 comparison of M1, M2 and Expt. spectral density (cm^2.s) Vs frequency (Hz)

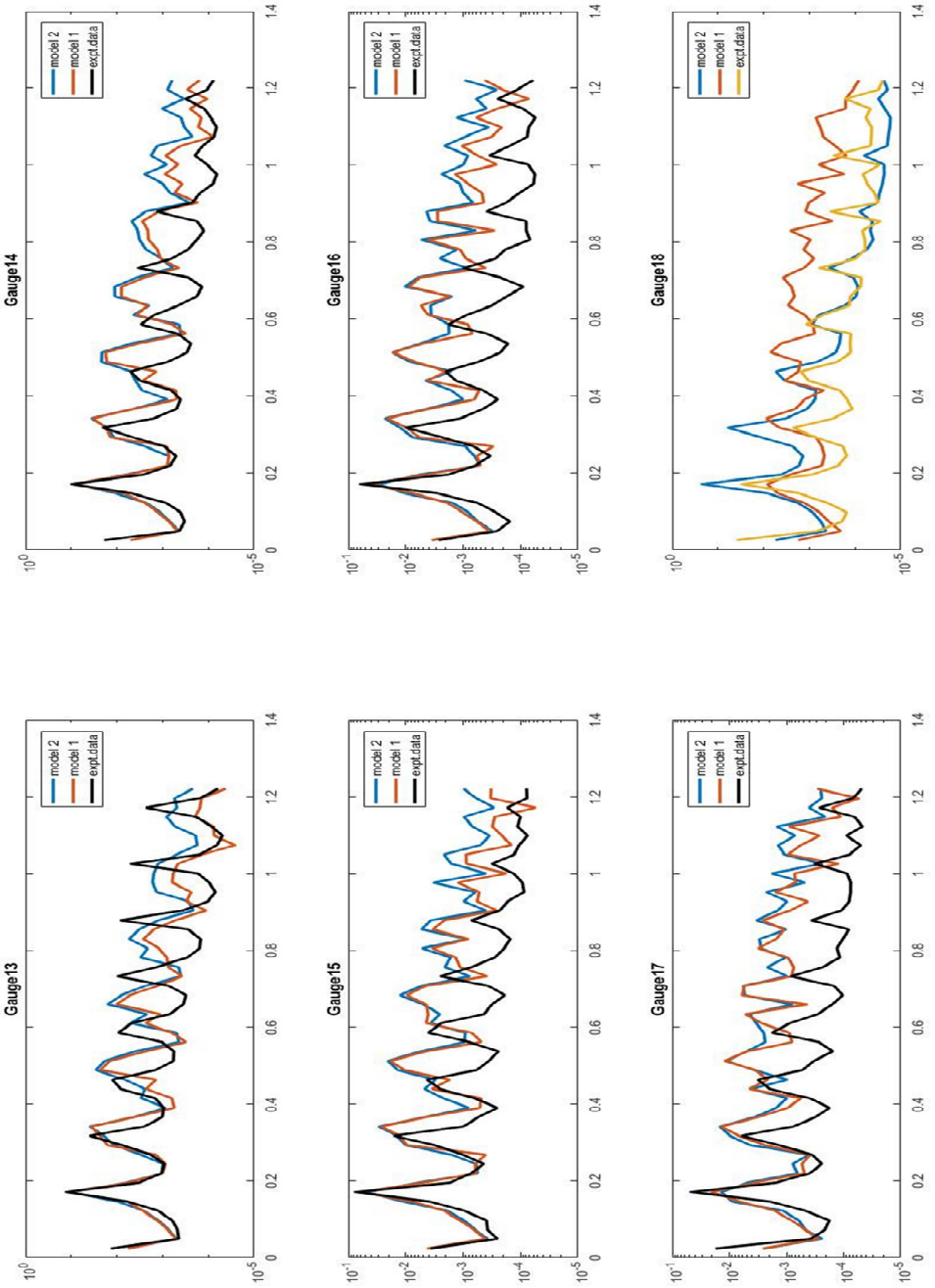

Gauge 13-18 Trial 1 comparison of M1, M2 and Expt. spectral density (cm^2.s) Vs frequency (Hz)

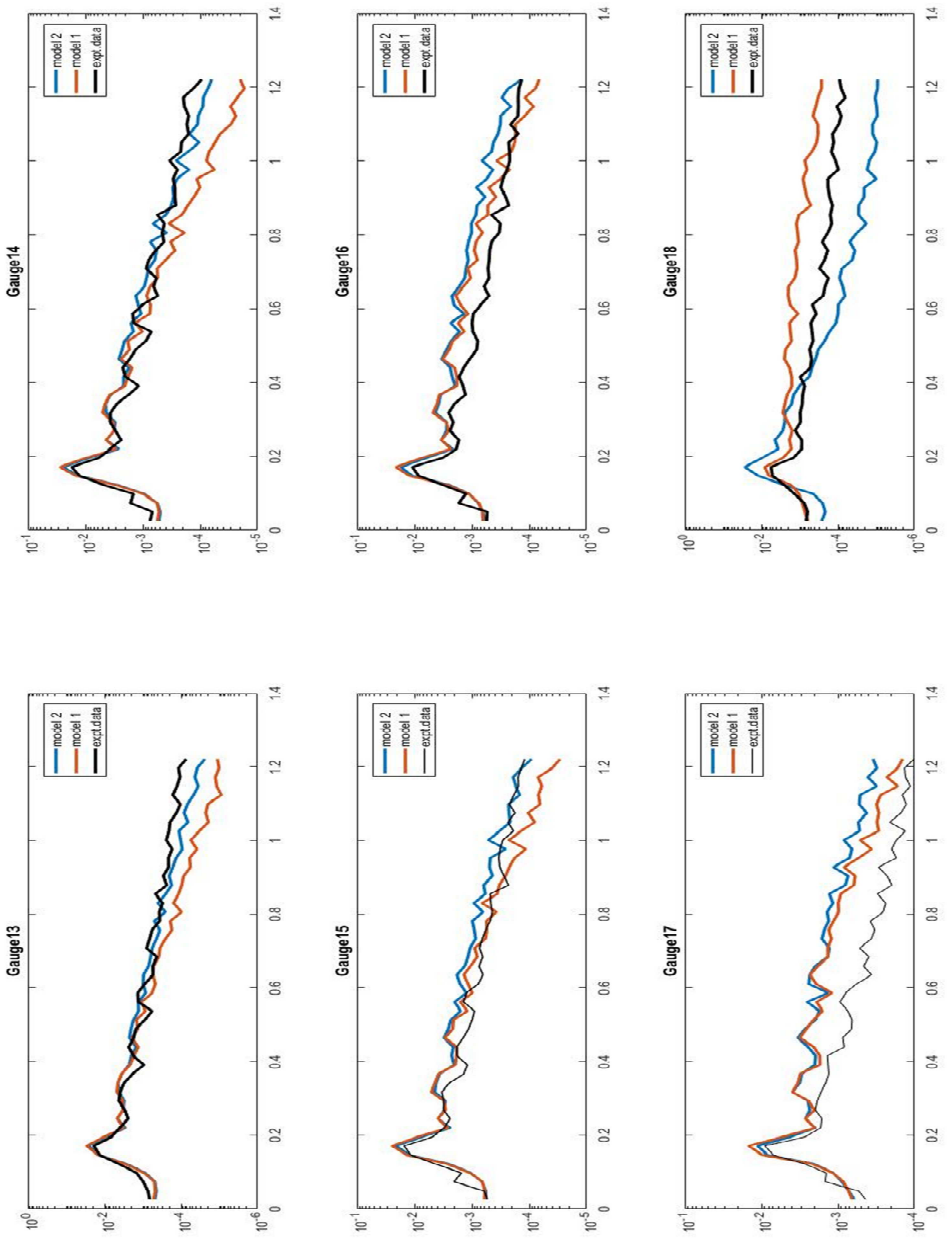

Gauge 13-18 Trial 2 comparison of M1, M2 and Expt. spectral density (cm^2.s) Vs frequency (Hz)

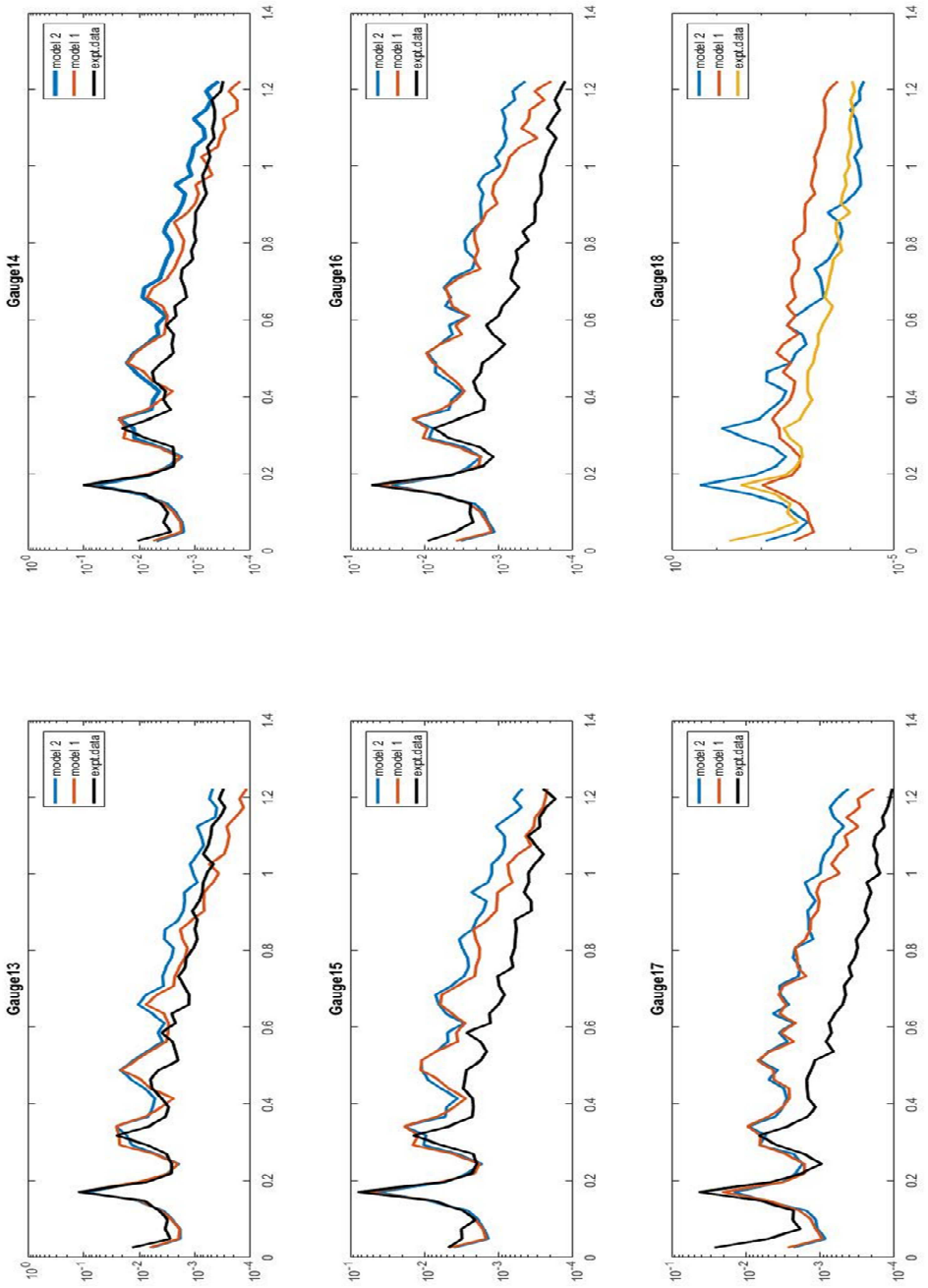

Gauge 13-18 Trial 5 comparison of M1, M2 and Expt. spectral density (cm^2.s) Vs frequency (Hz)